Università Politecnica Delle Marche

Department of Industrial Engineering and Mathematical Sciences

Faculty of Engineering

Master's degree in biomedical engineering

DESIGN AND IMPLEMENTATION OF A TEST BENCH FOR MEASUREMENT AND CHARACTERIZATION OF AORTIC VALVE BEHAVIOUR

Thesis advisor:

Prof. Lorenzo Scalise

Candidate:

Alice Ceccacci

Thesis supervisor:

Prof. Paolo Castellini

Academic Year 2022–2023

Index

Chapter I

1. Introduction

Cardiac disease is a significant global health concern, and its incidence has been increasing in recent years. According to the World Health Organization (WHO), cardiac disease is the leading cause of death worldwide, accounting for nearly 18 million deaths annually. The incidence of cardiac disease varies depending on various factors, including geographic location, age, sex, lifestyle, and genetic predisposition. Cardiac diseases encompass a wide range of disorders, including heart valves malfunctioning, leading to conditions such as valvular stenosis or regurgitation. These conditions can cause symptoms like shortness of breath, chest pain, and fatigue. When the severity of valve disease reaches a point where it significantly impairs heart function, valve replacement surgery should be performed. To validate prosthetic heart valves, several tests are typically conducted to assess their performance, durability, and safety. These tests aim to ensure that the prosthetic valves meet the required standards and can function effectively within the human cardiovascular system. In the field of research, the definition of experimental setups that allow to reproduce the conditions to which the heart valves are subjected is progressively increasing. The aim of these analyzes is the definition of a model that faithfully reproduces the cardiac activity and allows to validate the integrity of the valve prostheses. These investigations are led to the design of cardiac simulators. These simulators recreate the hemodynamic conditions and simulate the behaviour of the heart to assess the goodness of prosthetic heart valves. In this scenario, this thesis, carried out at the Dipartimento di Ingegneria Industriale e Scienze Matematiche, has as its main objective the validation of an experimental test bench that reproduce the cardiovascular system (ventricular) for the hemodynamic characterization of prosthetic aortic valve. The test bench for the cardiac simulator consists of a set of components that reproduce the anatomy of the heart organ (in particular the left ventricle and the aorta). The model of the human circulator is connected to a pumping system that generates and controls the flow of blood- mimicking fluid

within the simulator. Pressure sensors and flow meters are integrated into the test bench to measure and monitor the pressures generated within the simulator and the flow rates of the blood-mimicking fluid passing through the system. These sensors provide real-time feedback on the pressure profiles across the valves and within the simulated cardiovascular system. The aim of the present work thesis is to implement a LabVIEW control system that controls the piston pump and reproduce the pulsatile flow of blood and prove the goodness of the system by analyzing the generated pressure and volume waveforms. The tests conducted involve both a validation of the pumping system and a validation of the pressure and flow waves generated by the system. It ensures that the generated signals reproduce cardiac conditions and thus can be used to test the integrity of heart valves intended to replace diseased heart valves.

1.1 The heart: anatomy and physiology elements

The cardiovascular system is responsible for the supply of metabolic substrates (oxygen and nutrients) through the body and the removal of metabolism's by products. It is made of two branches: the pulmonary circulation, where the blood is enriched of oxygen, and systemic circulation, which distributes the blood to all the human organs. The heart and blood vessels are the primary components of this complex system. The heart's rhythmic contractions pump the blood through the vasculature and ensure that adequate blood flow is delivered to all living organs.[3][4].

1.1.1 Functional anatomy of the heart

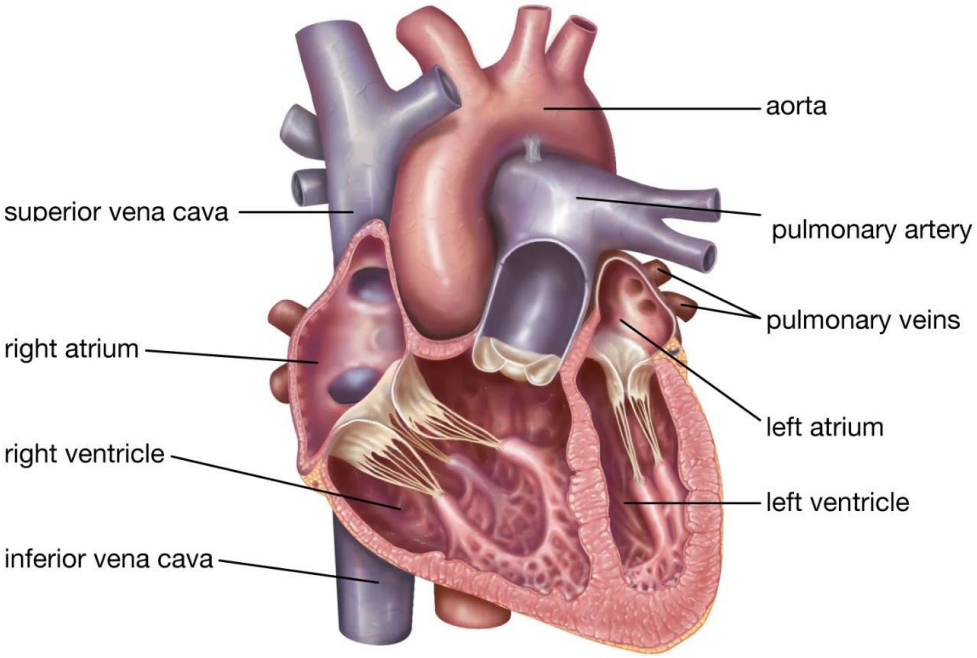

Figure 1: Anatomy of the heart.

The heart (Figure 1) is divided into a left and a right heart, in turn, subdivided into two chambers. The upper chambers are called atria and the lower chambers are called ventricles. The atria are low-pressure chambers, characterized by thin musculature, and act as reservoirs for blood flowing into the heart and as conducts toward their respective ventricles. The ventricles have thicker muscular walls to act as pumping chambers to propel blood outside the heart.

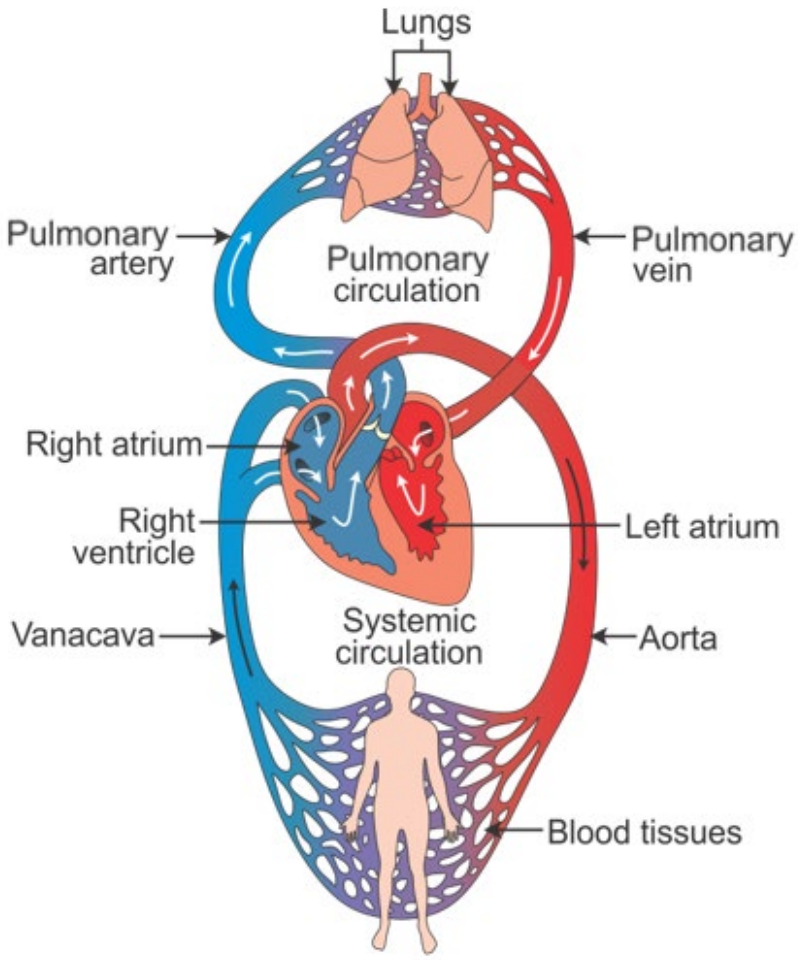

Figure 2: Heart and blood circulatory system.

The right atrium is connected with the superior and inferior vena cava, which carries deoxygenated blood from the systemic circulation (Figure 2). The blood enters through the atrioventricular valve the right ventricle and is ejected into the pulmonic artery which carries the blood into the lungs. There, it takes place the exchange of oxygen and carbon dioxide. The left atrium receives oxygenated blood by way of the pulmonary veins coming from the pulmonic circulation. Blood passes through the atrioventricular valve into the left ventricle. As the left ventricle contracts, blood is ejected outside the heart through the aorta, from which it is delivered to the human body. The systemic circulation provides the functional blood supply to all body tissue. It carries oxygen and nutrients to the cells and picks up carbon dioxide and waste products.

1.2 The cardiac cycle

The cardiac cycle is the complete sequence of heart mechanical events. It consists of systole and diastole phases. During the diastole, the heart relaxes and fills with blood. During the systole the heart muscle contracts and blood ejection takes place. The events that occur throughout an entire cardiac cycle should be described with the Wiggers diagram. The Wiggers diagram (Figure 3) depicts the electrocardiogram trace (ECG), pressure, and volume change in the left side of the heart, hearts sound as a function of time during a complete cardiac cycle.

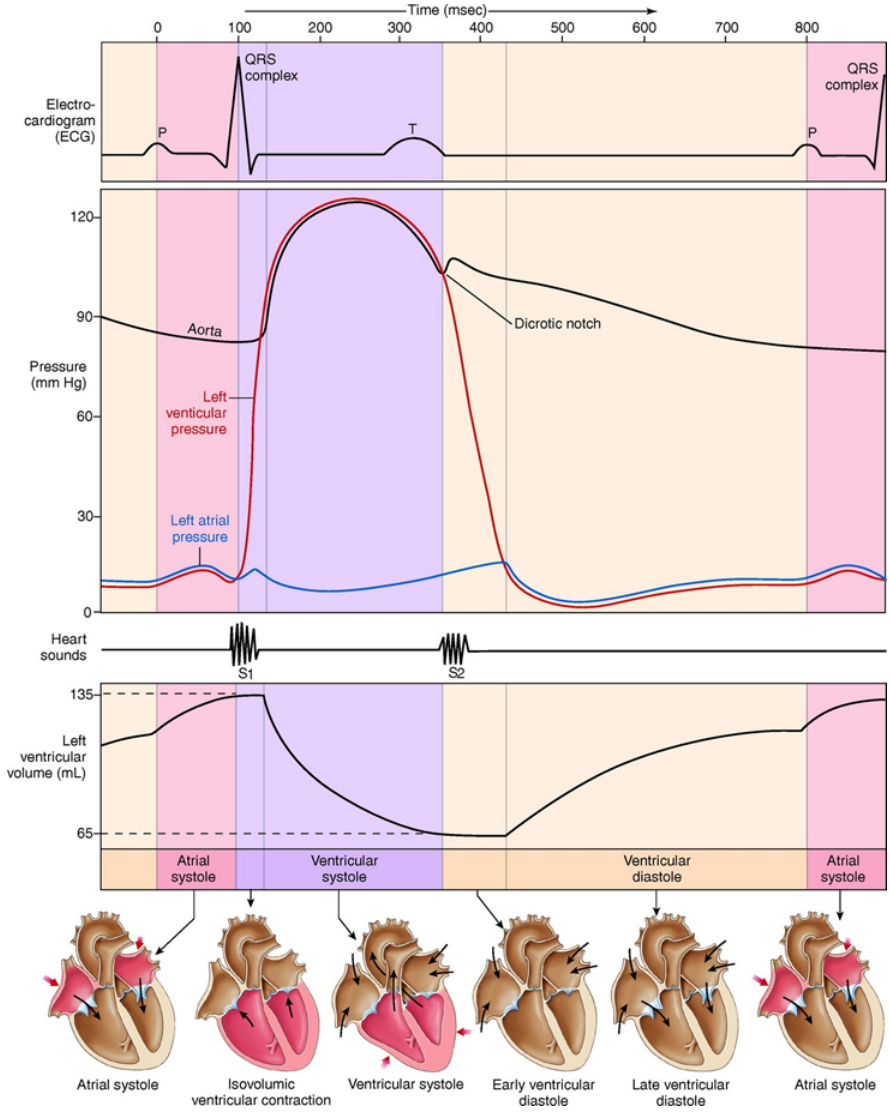

Figure 3: Wiggers diagram: Electrocardiogram, pressure, heart sound and left ventricular volume, in time[ms].

The first phase of the cardiac cycle is the atrial systole, which corresponds to the atrial musculature contraction because of the depolarization of the atria indicated by the P wave of the ECG. In this phase the atrial pressure increases leading to blood flowing into the ventricles. The flow of blood from the atria that takes place in this phase completes the ventricular filling. At the end of this phase, which corresponds to the end of ventricular diastole, the left ventricular end-diastolic volume (EDV) is about 120 mL (associated with an end-diastolic pressure (EDP) of about 8 mmHg). The ventricular systole is initiated by the ECG QRS complex, which represents ventricular depolarization. The ventricular contraction leads to a rapid increase of the ventricular pressure, leading to the closure of the atrioventricular valves. The atria ventricular valves closure coincides with the first heart sound (S1). The interval between the start of ventricular systole and the opening of the semilunar valve is called isovolumic ventricular contraction because, during this brief phase, no change in ventricular volumes occurs. The intraventricular pressure rise causes the semilunar valve to open. Then blood is ejected outward from the heart into the pulmonary artery and into the aorta. The first phase of the ejection is characterized by maximal outflow velocity, maximal aortic (120 mmHg) and pulmonary artery (25 mmHg) pressure. While the blood is flowing outside the ventricle, the ventricular volume is decreasing, as well as the atrial volume is increasing due to the blood flow coming from the pulmonary vein and superior and inferior vena cava. The phase that follows this rapid ejection is characterized by a progressive reduction in the outflow velocity. At the end of ventricular muscle contraction, the ventricular pressure abruptly falls and the aortic and pulmonary artery valves close, producing the second heart sound (S2). The semilunar valves closure indicates the systole end and the diastole begin. Ventricular diastole may be divided into an earlier phase (early ventricular diastole) and a second (late ventricular diastole). During early ventricular diastole, both semilunar and atrioventricular valves are closed. This is the phase of the cardiac cycle in which the ventricles are filled with the lowest volume of blood ever (about 50 mL). The volume of blood remaining in the ventricle after contraction is called the end-systolic volume (ESV). The

stroke volume, the amount of blood ejected outside the heart at the end of the ventricular systole, is equal to the difference between end- diastolic volume and end-systolic volume. The gradual increase in the atrial pressure determines the opening of the mitral and tricuspid valves. Once the atrioventricular valves open, the blood that had filled the atrial chamber during the ventricular systole is flowing toward the ventricle. Then, during late ventricular diastole, the left atrium and right atrium contractions determine the end of ventricular chamber filling.

1.2.1 Ventricular pressure-volume relationship

The left ventricular pressure-volume relationship is a fundamental concept in cardiac physiology that characterizes the changes in pressure and volume within the left ventricle throughout the cardiac cycle. The graphical representation of the pressure and volume changes over time is called the left ventricular pressure-volume loop (Figure 4). It is a closed-loop curve that starts at the EDV, goes through isovolumetric contraction, ventricular ejection, isovolumetric relaxation, and returns to the EDV for the next cardiac cycle. The loop provides valuable information about the mechanical function of the left ventricle, including stroke volume (the difference between EDV and ESV), ejection fraction (the fraction of EDV ejected during systole), and cardiac output (the volume of blood pumped by the ventricle per minute). In the pressure-volume loop, the relationship between the left ventricular volume and the pressure within the ventricle during diastole is represented by the End-Diastolic Pressure-Volume Relationship (EDPVR). It characterizes the ventricular compliance, or the ability of the ventricle to stretch and accommodate blood during filling. The steeper the slope of the EDPVR, the less compliant the ventricle. This relationship is influenced by factors such as myocardial stiffness, fibrosis, and hypertrophy.

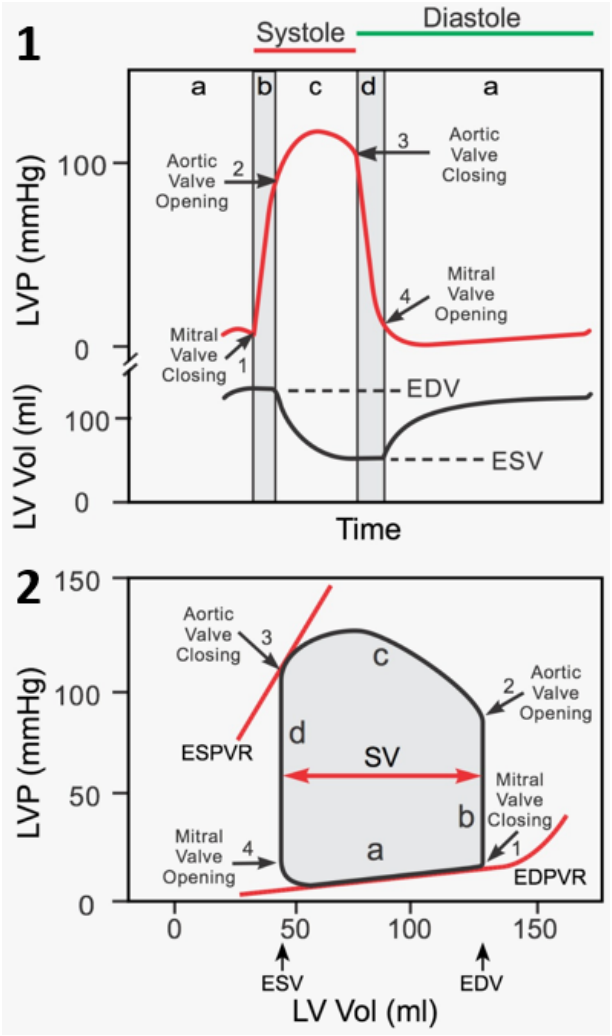

Figure 4: Left ventricular pressure and left ventricular pressure through a cardiac cycle. [2] Ventricular pressure-volume loops. (a) ventricular filling, (b) isovolumetric contraction, (c) ventricular ejection, (d) isovolumetric relaxation.

Changes in the EDPVR can reflect alterations in ventricular function and can be useful in assessing diastolic dysfunction. The End-Systolic Pressure-Volume Relationship (ESPV), on the other hand, represents the relationship between the left ventricular volume and the pressure within the ventricle during systole. It describes the ventricular contractility, or the strength of the ventricular muscle contraction. The ESPVR slope is known as the end-systolic elastance, which is a measure of contractile performance. An increased slope of the ESPVR indicates enhanced contractility, while a decreased slope suggests reduced contractile function. Overall, understanding the left ventricular pressure-volume relationship and the associated pressure-volume loop is crucial in assessing cardiac performance, diagnosing heart conditions, and guiding therapeutic interventions.

1.3 The cardiac valve

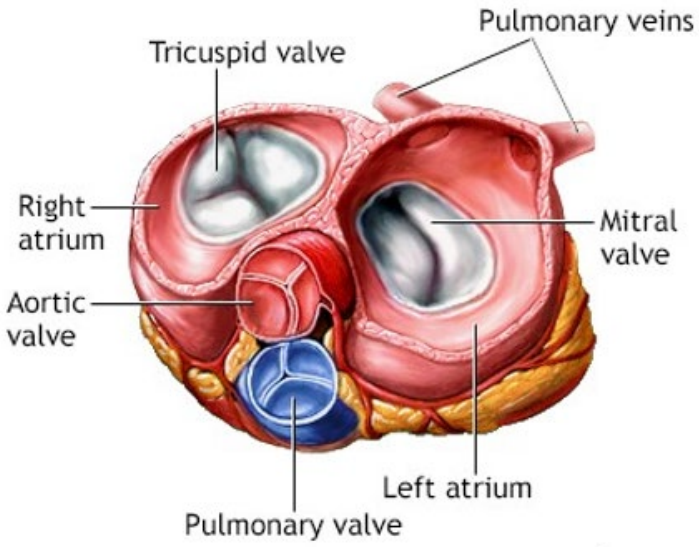

Figure 5: Heart valves.

The cardiac valves (Figure 5) ensure unidirectional blood flow. They consist of fibrous connective tissue covered by the endocardium. The atrioventricular valves lie between the atria and the ventricle. Those are attached to papillary muscles located on the left and right ventricles by chordae tendineae. This attachment prevents the valves from leaking blood into the atria during ventricle contraction. The tricuspid valve, made up of three cusps, lies between the right atrium and the right ventricle. The left atrium and left ventricle are separated by the mitral valve, which is made up of two cups. Semilunar valves connect ventricles with outflow arteries. They are attached to the wall of the pulmonary artery and aorta and are made up of three cups attached to the valve rings. The pulmonary valve is located between the right ventricle and the pulmonary orifice while the aortic valve lies between the left ventricle and the base of the ascending aorta. They close at the end of the ventricular diastole, preventing the backflow of blood into the ventricles.

1.3.1 Prosthetic heart valve

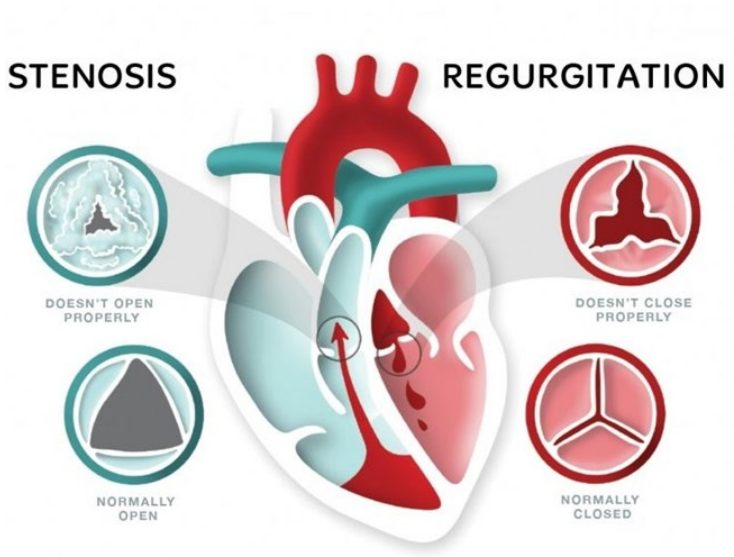

Figure 6: Cardiac valves disease. Pulmonary regurgitation and aortic stenosis.

Cardiac valve disease should be classified into two main categories: valvular stenosis and valvular regurgitation (Figure 6). Stenosis is a pathological condition characterized by a narrowed valve orifice. In contrast, valvular regurgitation is the condition in which a heart valve does not close properly. A diseased valve, either affected by regurgitation or stenosis, would cause hemodynamic compromise or affect the quality of life and will often warrant evaluation regarding possible prosthesis. Both pathological conditions can be characterized by a different degree of severity. In certain conditions, the treatment of severe stenosis or severe regurgitation should involve the injured valve replacement with a prosthetic heart valve. (Figure 7) [6].

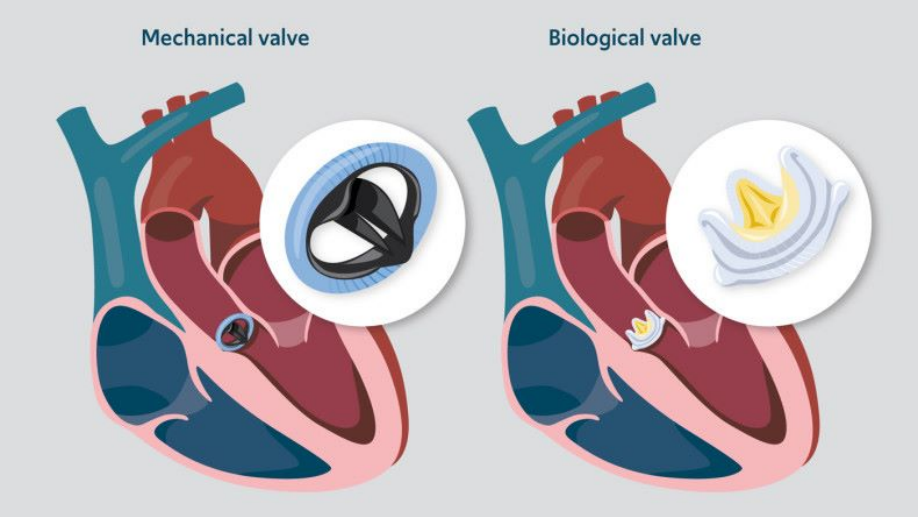

Figure 7: Mechanical and biological aortic prosthetic valves

The European Society of Cardiology reported that over the past 50 years have been performed about 4 million prosthetic heart valve (PHV) replacements and that this procedure represents the only definitive treatment in case of severe cardiac valve disease. By the end of 2050, this overall number is going to be 850000 [5]. Replacement valves should be broadly grouped as biological or mechanical.

1.3.2 Mechanical heart valves

The mechanical heart valves (Figure 8) are made up of synthetic material. The constituent components of these valves are an occluder, an occluder constraint, and a suture ring. Over the years the design of mechanical valves has evolved, starting from the first prototype of Hufnagel of the 1940, to the more recent and improved solutions. Currently, synthetic valves fall into three general categories: caged ball valves, disc valves, and bileaflets valves. Pyrolytic carbon (PyC) is the most widely used structural material for mechanical heart valves due to its biocompatibility, low cost and ease of manufacturing.

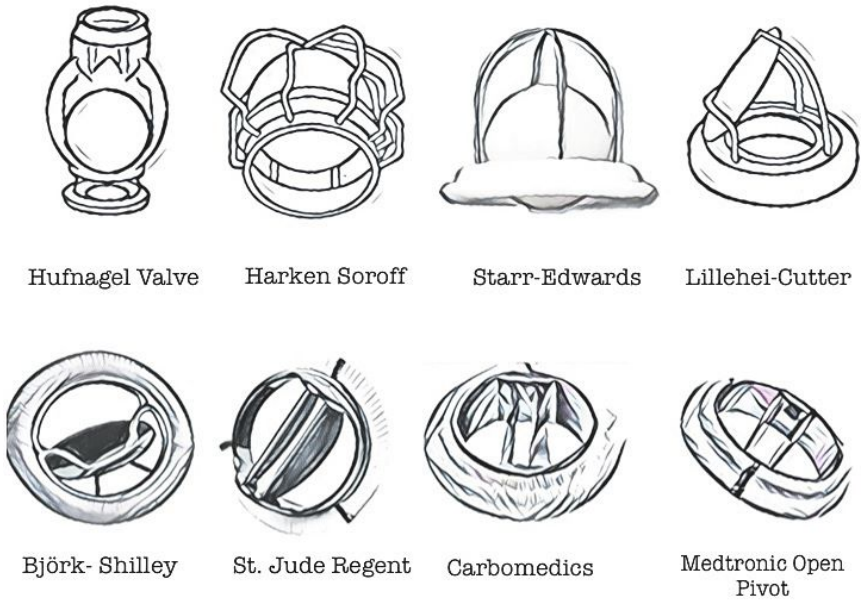

Figure 8: Mechanical heart valve evolution. [8]

These valves have the longest longevity, indeed can last up to 20-30 years. However, their major drawback is the high thrombogenicity, due to the carbon release into the blood, and for this reason, they are not always the best alternative in the need of heart valve replacement. The first prototype of artificial heart valve, designed by Hufnagel in 1952, is the caged ball valve. It consists of a sphere housed inside a cage. During heart contraction, the blood pressure pushes the ball against the cage and thus allows blood to flow. A first example of improvement of its design is represented by the Harken-Soroff prototype (1960). To overcome the side effects related to these first prototypes, several improvements have been applied to these designs. The caged ball valve that is the result of this continuous improvement is the Starr-Edwards valve. This valve was introduced in 1960 and is the caged ball valve with better hemodynamic properties. The key element of this valve is a silicone ball enclosed within a titanium cage. Over the years it undergoes several changes in materials and shape. It was retired in 2007 due to its poor hemodynamic properties and the insurgency of side effects and the spread of better-performing replacing valves.

Historically, the tilting-disc valve is the second design of a mechanical valve. This valve is constituted by an occluder controlled with a metal strut. The circular occluder is attached to a structure that holds a mechanism made up of two disks that open and close to allow blood passage. The first prototypes of the tilting-disk valve were developed by Lillehei in 1959 and Bj¨ork-Shiley in 1960.

The innovation in prosthetic valve development leads to the introduction of the bileaflets valve starting from 1970. Bileaflets valves are made of two semicircular leaflets attached to a rigid ring by small hinges. The rotation of the semilunar disks allows blood flow. These valves, realized in pyrolytic carbon, are characterized by a better blood flow profile compared with the previous mechanical heart valves. Due to their hemodynamic profile and the low incidence of thrombosis, those are the most commonly used mechanical prosthesis today. Some examples of this category are the St. Jude Reagent valve (1977), the Carbomedics bileaflets mechanical prosthesis (1986), and the Medtronic Open Pivot heart valve (1992).

1.3.3 Biological heart valve

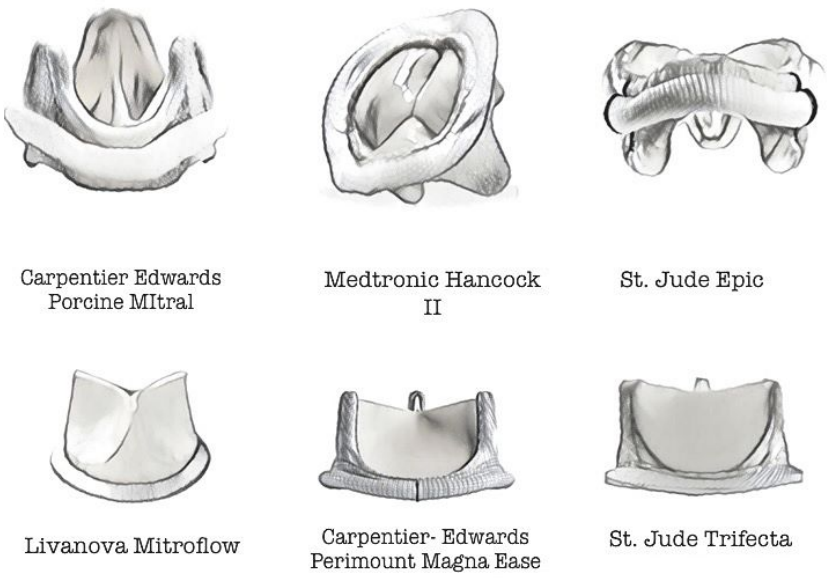

Figure 9: Biological heart valves evolution. [8]

Biological heart valves are made up of animal tissue attached to a metal o polymer support (Figure 9). These should be made of animal (xenografts) or human tissue (allografts/homografts). Depending on their design, these should be grouped as stentless or stended. Stentless surgical valves are most often constructed from porcine or human aortic root tissue.

Although stentless valves tend to have more laminar flow and lower transvalvular gradients than stented valves, increased durability has not been demonstrated. Stented valves are usually constructed with bovine pericardium or whole porcine aortic valves attached to a support structure such as a stent or frame to facilitate implant, maintain 3D relationships, and more physiological flow.

Xenogenic heart valves of animal origin (usually bovine or porcine) are based either on animal heart valves or animal pericardial tissue, and differ on the nature, type of construction, and chemical fixation. Some examples of widely used stented porcine heart valves are the Carpentier Edwards (1975), the Medtronic Handcook II (1980), and the St. Jude Epic (2003). Examples of stented pericardial bovine valves bioprostheses are the Carpentier Edwards Perimount Magna Ease (1981), the Livanova Mitroflow (1982) and the St. Jude Trifecta (2007). These solutions are used for the replacement of both native or prosthetic aortic valves or mitral valves. Biological heart valves can be obtained also from human donors, derived both from human donors or from the patient's own tissue. Allograft valves are harvested from cadavers or heart transplant recipients. These prove to have significant resistance to infection and have enhanced physiologic hemodynamical properties. Autograft heart valves using of an autologous pulmonary valve to recon- struct the diseased aortic or mitral valve has been proposed by Ross in 1967. In contrast to mechanical valves, the biological heart eliminates the usage of anticoagulants, but the lifespan of tissue valves is usually less than 15 years, and the patients may need to go through multiple thoracic surgeries. For this reason, these valves are suggested for elderly patients.

1.4 Transcatheter aortic valve implantation

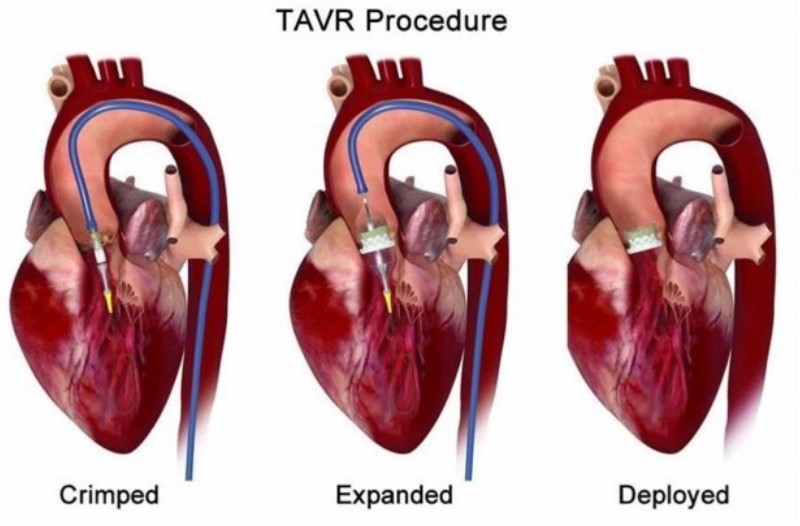

Figure 10: Tavi procedure. Baloon catheter is inserted thought aorta into heart valve. Then transcatheter valve placed into position over the diseased aortic valve.

The Surgical Aortic Valve Replacement (SAVR) is the gold standard to perform aortic stenosis replacement. This procedure consists of the complete substitution of the injured valve with open-heart surgery to implant a prosthetic valve. To overcome the invasiveness of this procedure and the complications that it might imply, in the last decade SAVR is going to be overcome by the minimally invasive Transcatheter Aortic Valve Replacement (TAVR), sometimes called Transcatheter Aortic Valve Implantation (TAVI). TAVR is an alternative to open-heart surgery performed by delivering a bioprosthetic valve in a crimped configuration through a catheter, usually inserted in the transfemoral vessel (Figure10). The vessel is mounted over a metallic stent so that when it reaches the correct position it expands (using balloon inflation or self-expanding stents) inserting the replacing valve into the aortic root, pushing the native leaflets without their removal. While conventional open-heart SAVR procedure can consider the presence of calcium deposits before of replace the injured AV, Transcatheter Heart Valve (THV) displacement might against calcification alter the THV kinematics. The concept of TAVI is relatively recent. The first study was

performed starting in 1989 in Aarhuus University Hospital Denmark, coming up with the first-in-human implantation in 2002. Starting from that moment, this procedure has been subjected to considerable expansion that leads the Food and Drug Administration (FDA) to approve the TAVR to surgical valve replacement in inoperable patients (in 2011) and operable high-risk patients (in 2012). Nevertheless, the increasing interest in this technology would in the future made it the preferred solution also for low-risk patients. The THV approved by the FDA are the Edwards SAPIEN family balloon-expandable valves and the Medtronic's Core Valve self-expandable valves. In addition to interventions that require the replacement of the native injured aortic valve, recently the TAVR devices have been used to replace the failing valve previously implanted with either SAVR or TAVR surgery, being involved in a so-called Valve-in-valve (ViV) procedure. The growth of valve-in-TAVR (ViTAVR) procedures requires dedicated THV devices, to carry out free of complications AV replacement. Limited studies reported a comparison between ViTAVR and valve-inSAVR (ViSAVR), the one carried out by Reschipichler et al. showed that compared with ViSAVR, ViTAVR should be a considerable choice, providing sliding better hemodynamic and similar success rate [7]. Despite the success of the TAVR device, this procedure is not yet free of complications. Some of the common complications are bleeding, stroke and heart attack. Those problems are associated to the presence of calcific material where the valve is inserted, but also to wrong displacement. The major fluid mechanics related failure involves paravalvular leak, a common complication that refers to blood flowing through a gap between heart tissue and implanted valve, resulting from inappropriate sealing [7]. The solution to overcome this matter is to design a device able to minimize paravalvular leak ensuring better adhesion of the implanted valve on the heart tissue. An example is the one adopted by the SAPIENS3 design includes a PET fabric skirt for better attaching the stent to the aortic root. Apart from mechanical failure that could arise from improper THV displacement, another important reason for THV failure that limits the applicability of TAVR to the younger population is the degeneration of the biological leaflets, compromised also by crimping-induced damage that contributes to reduce the valve long-term durability in vivo. Indeed,

the American Heart Association and American College of Cardiology (AHA/ACC) guidelines state that biologic valves are the preferred choice in patients aged 70 or above, while a mechanical valve is reasonable for patients below 60 years of age. The material that could be a good candidate to replace the xenographic material is the polymer. Despite several polymers that pass the ISO durability tests, there is still no polymer-based valve approved by the FDA to perform TAVR. Moreover, biological heart valves, are more commonly used in TAVR procedures because of the challenges associated with the delivery system used in TAVR. Indeed, the rigid structure of mechanical valves can make it difficult to compress and deliver through a catheter. Hydrodynamical validation of THV is guided by ISO 5840-3, which determines with accuracy the in-vitro testing procedure to validate efficacy and safety for FDA approval. These tests are used to ensure the physical, biological, and mechanical properties of prosthetic valves, and are performed using devices that simulate the hydrodynamic of native aortic valve. While ISO 5840-3 defines the testing procedures, the need for investigating alternative solutions imply the definitions of newer testing methods implemented in accordance with the ISO standard to perform a deeper evaluation of THV device. These are performed using computational or experimental models and involve patient-specific models that allow an examination of THV device in a very realistic anatomical scenario, for improving THV testing and design.

1.5 Cardiac simulators: State of the art

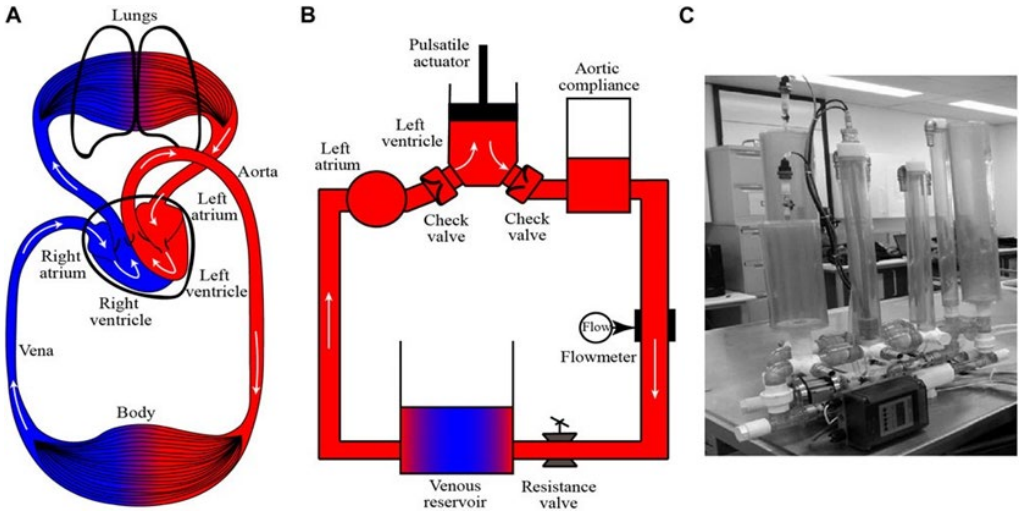

Figure 11: Illustration of (A) human cardiovascular system, (B) one basic MCL with systemic circulation and (C) one example of MCL [10].

The mock circulatory loop (MLC) or cardiac simulator is an experimental set-un reproduction the cardiac system and that makes it possible to evaluate the goodness of implantable devices. Due to the high rate of cardiovascular diseases, the design of such kind of devices has gained a progressive interest. One of the major reasons for the spread of cardiac simulators is the possibility of evaluating the goodness of a large range of cardiac implantable devices without the need of performing in vivo evaluation. In addition, an experimental setup based on a cardiac simulator is less expensive, gives the chance to perform a higher number of tests and evaluation, and allows to perform of easier control experiments with high repeatability. The Figure 11 depicts the basic principle under the design of a cardiac simulator. The illustration compares the basic model of the cardiac simulator with the human cardiac system and a real cardiac simulator.

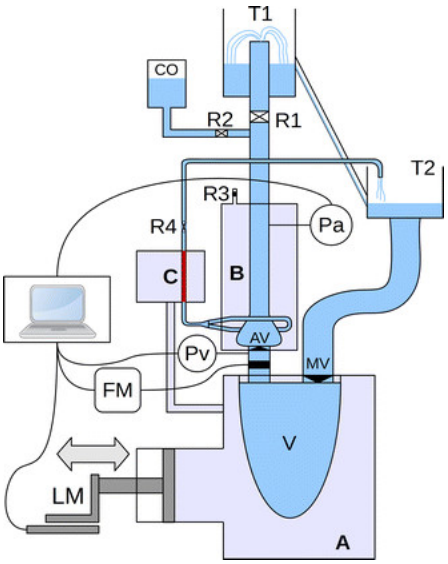

Figure 12: Schematic model of the cardiac simulators from the study of Querzoli et al. [11].

These devices indeed have been invented to reproduce the human cardiac system following a hydraulic closed-loop model realized as a set of reservoirs and valves having the same feature that characterize the cardiac system organs. The first prototype was invented in 1950 by McMillan and its colleagues. Their prototype consists of only a ventricular chamber and was employed to carry on studies on heart valve movements. Since the first prototype, after almost seventy years, various studies have been conducted to improve the cardiac simulator quality to obtain a cardiac system model as similar as possible to the human cardiac system (Figure 12). In these terms, research have been conducted with various prototypes to define the best design and the best materials, capable of reproducing the organs constituting the cardiac system in the more accurate way. The purpose of these analyses is to improve the response of the simulator when applied external stimulations that reproduce the stimulation to which the heart is subjected and by monitoring the pressure and flow waves generated.

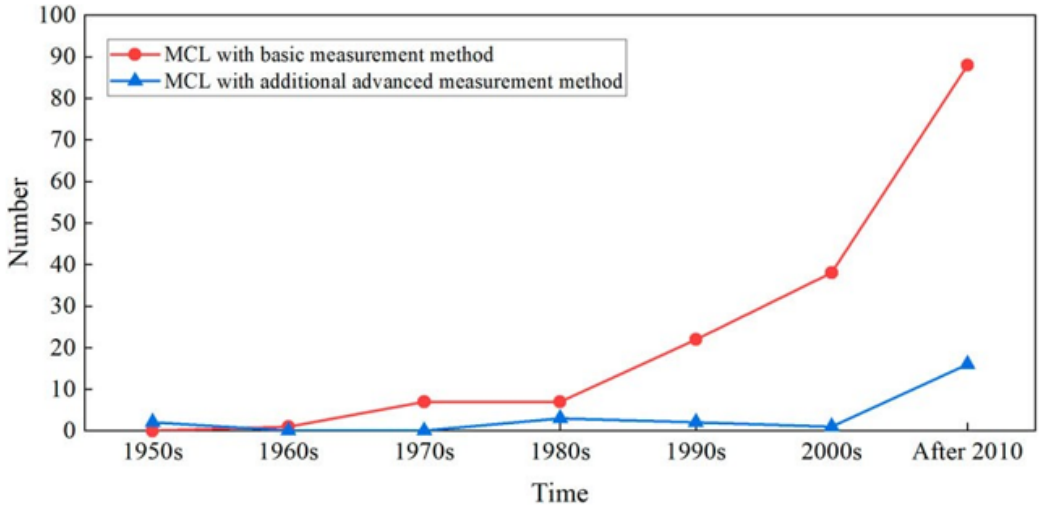

Figure 13: The number of the MCL and its measurement method changes over time, according to the references of this article statistically. The basic measurement method includes pressure, flow measured from the transducers. The advanced measurement method includes

The progressive interest in such kind of technology is depicted in figure 13, where it is possible to appreciate how the number of studies has increased in the last decade.

In the cardiac simulator prototyping, the left ventricle is modelled by a rigid reservoir subjected to the stimulation applied by linear actuator.

The figure 14 summarizes some of the constituent elements of cardiac simulators. The cardiac cycle events (systole and diastole) and the heart rate are simulated by the pulsatile movement of the motor. The ventricle systole, diastole and heartbeat can be simulated by the motor stroke and frequency. Alternatively, the left ventricle should be modelled using an elastic sac pump driven. The simulator includes aortic valve, in the outflow tract of the left ventricle chamber, and should include mitral valve in the inflow tract of the left ventricle. Industrial or medical valves can be chosen to be placed within the simulator. The aortic arch is simulated by another chamber with compliance emulate the compliance of the human aorta, and it is essential to regulate the flow ejected from the left ventricle. The cardiovascular system peripheral resistance is generally simulated by a resistance valve and realized by a third reservoir. Depending on the complexity of the model, left atrium and vena cava can be modelled as one reservoir. As working fluid, a water/glycerine mixture is generally used due to its density

(1.060–1.100 kg/m3) and dynamic viscosity (3.5–3.6 cP), similar to that of the blood, and due to its optical properties. One of the more common applications of pulse duplicator is testing of physical, biological, and mechanical properties of prosthetic valves before implantation. To perform such kind of evaluation pressure and flow parameters are monitored, because these quantities ensure the validation of heart valve mechanics. Despite all the advantages that offers the cardiac simulator, that ensure to simulate various physiological and pathological conditions, these devices suffer of the limitation that characterize the in vitro experimentation and the impossibility of fully mimicking the human circulatory system. In fact, the movement of the ventricle is limited because in the simulator the reduced flexibility in the ventricle does not allow to replicate the ventricle torsion that occurs during the cardiac cycle. Moreover, it is not possible to properly replicate the Frank-Starling response in some simulators. Indeed, it is not possible to fully model the mechanism that regulates the contraction of the heart according to the ventricle. due to the passive ventricle filling in cardiac simulator. These limitations of the in vitro experiments are reflected in a certain degree of difference from the native value of some parameters such as aortic and left ventricle pressure or the cardiac output.

Organs in CVS	Models in MCL	Advantages
Ventricle	Rigid chamber with a linear motor (Tuzun et al., 2011; Ruiz et al., 2013; Bozkurt et al., 2016)	Easily controlled and with swift response
	Flexible sac driven pneumatically (Wu et al., 2004a; Pantalos et al., 2004; Wang Y et al., 2017)	More native pressure curve can be obtained from this model than that from rigid chamber model
Aorta	Airtight container with air above (Westerhof et al., 1971; Feng et al., 2017; Gehron et al., 2019)	This model is easy to be built and the compliance is simulated by the compressibility of air
	Spring capacitor (Ferrari et al., 1994; Woodruff et al., 1997; Pantalos et al., 2004)	The compliance is simulated by the elasticity of the spring instead of the air, thus this model consumes less volume than the airtight container. Meanwhile, the compliance can be adjusted by changing the load on the springs
	Flexible tubes (Pantalos et al., 2010; Ferrari et al., 2011; Gräf et al., 2015)	The compliance is simulated by the elasticity of the flexible tubes. By isolating the fluid and air, this model avoids the influence of air on the test fluid. This model is more attractive in the experiment with blood such as the *in vitro* hemolysis test
Valves	Check valve (Khienwad et al., 2019; Gregory et al., 2020; Li S et al., 2020)	Cheap and good reliability
	Prosthetic or bioprosthetic valves (Koenig et al., 2004; Schlöglhofer et al., 2013; Stanfield and Selzman, 2013)	These valves have less pressure loss and better hemodynamic performance than that of the check valves

Figure 14: Organs in the cardiovascular circulation correspond to major components in MCL and their advantages.

Chapter II

2. Materials and methods

2.1 Laboratory setup and equipment

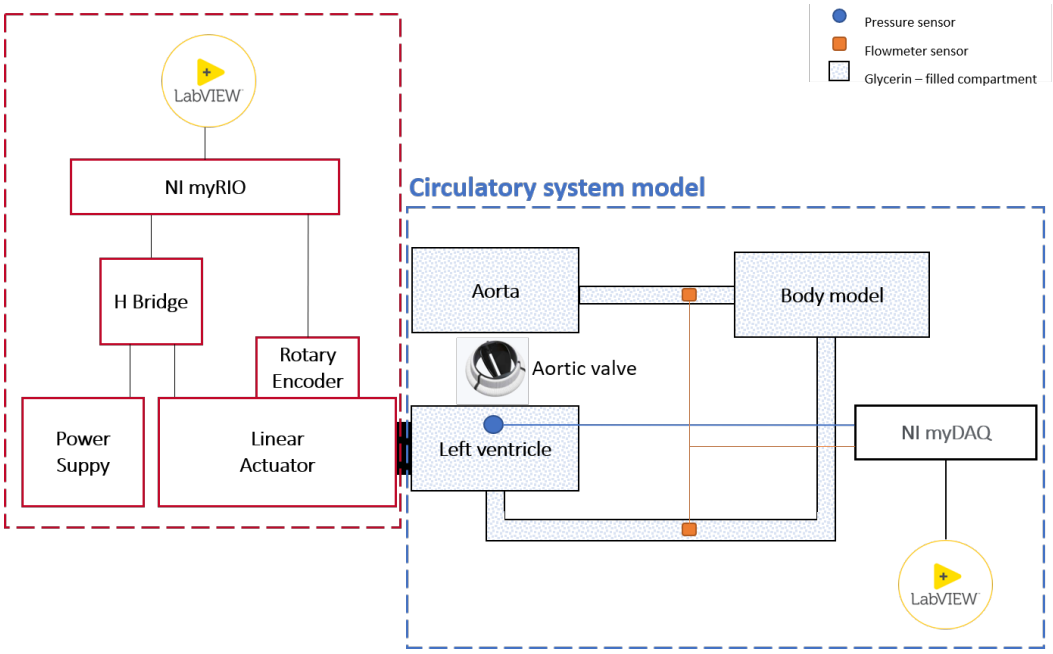

Figure 15: MCL scheme including schematic model of the cardiac simulator and control system.

The present work was carried out with MLC schematically, depicted in Figure 15, including a pumping device to simulate the variable cardiac preload, two reservoirs with elastic membranes that simulates left ventricle and aorta, and a more rigid peripheral artery system with embedded pressure and flow dynamic sensors. This closed-loop system is filled with water, a substance that simulate the blood in the circulatory system that is chosen for its optometric properties. A control system and a measurement system using LabVIEW 2011 (National Instruments) has been connected to the cardiac simulator to replicate ventricular operation and to acquire pressure and flow dynamic signal.

2.1.1 Human circulation model

The laboratory test bench (Figure 16) is composed by left ventricle model, pumping system, aortic arch and the body model tank.

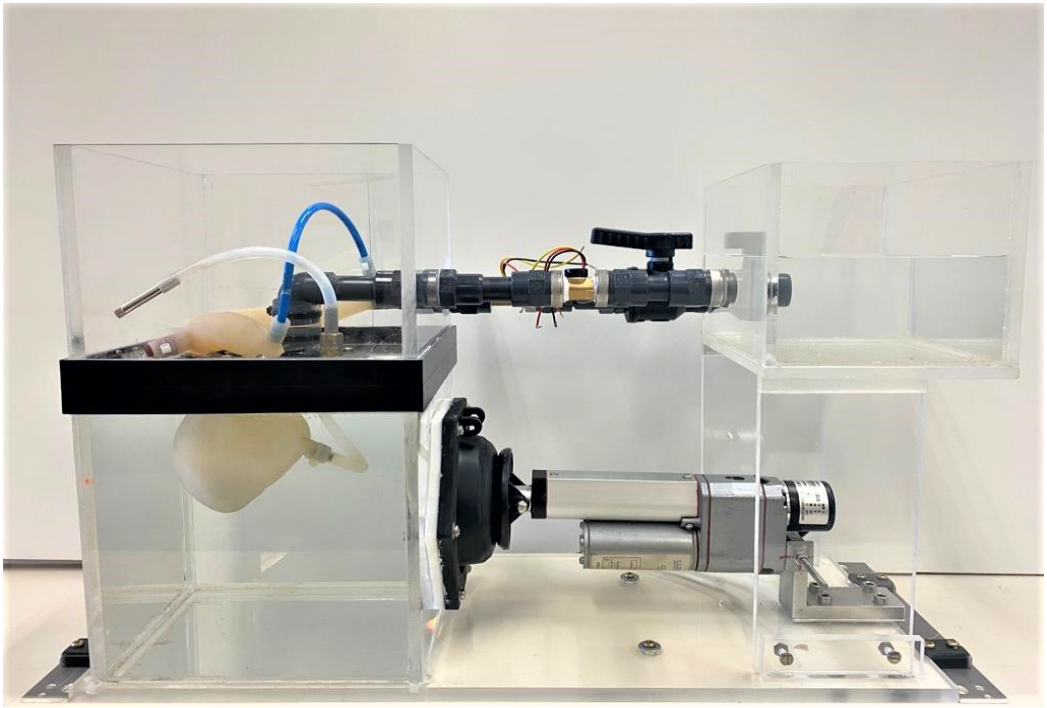

Figure 16: Laboratory test bench.

The left ventricular model is realized with an elastic membrane enclosed within a plexiglass tank. The plexiglass tank panel thickness is about 8 mm, the plexiglass tank size is 198 x 198 mm. The plexiglass tank has two holes to connect the 3D printed left ventricle (Figure 17) with an external pumping system and a reservoir that model the aortic arch. The left ventricular chamber is the starting point for the cardiac closed - loop system: the entire evolution of the system starts from the ventricular chamber, that is subjected to the action of the linear actuator and induce the liquid movement thought the entire system. The membrane compliance mimics the elastic properties of the natural left ventricle, so that an increasing pressure leads to the membrane dilatation. The rhythmic dilatation and relaxation of the ventricle membrane leads flow ejection into the

aortic arch across an aortic valve, that is a bileaflets mechanical valve. (Figure 18).

Figure 17: 3D- printed Left Ventricle

Figure 18:Aortic valve used in this test bench.

The aortic arch (Figure 19) is realized using a 3D printed highly elastic chamber that dilatate when receiving water from the left ventricle to propel it into a third plexiglass tank. The aorta is connected to the fluid reservoir with two rigid silicone tubes in place of the peripheral arteries. These parallels tubes are embedded with a measurement system which provide real time continuous monitoring of pressure measurements and fluid dynamic flowmeters. At this stage, the water that flows inside the fluid reservoir is ejected back into the left ventricle tank by the action of the mechanical pump.

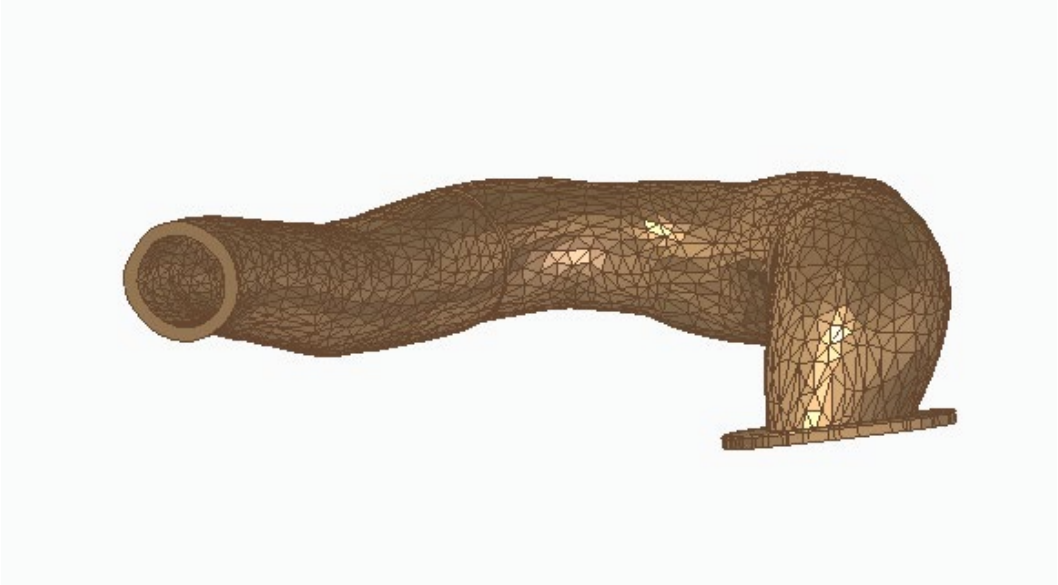

Figure 19: 3D-printed aortic arch.

2.1.2 Pumping system

The pulsatile activity of the heart has been simulated with a backward and forward movement of a pump that causes the ventricular membrane to have a linear displacement. This mechanism has been designed in a way to reproduce the mechanic of the ventricle through an entire cardiac cycle: when the pump pushes the ventricle membrane, the fluid present within the ventricular tank is ejected outside the ventricular chamber, simulating the blood ejection outside the heart that occurs during the systole. On the other hand, when the pump moves backward, the ventricular membrane moves in the opposite direction letting the fluid fill the ventricular chamber, simulating the ventricular filling that occurs during the diastolic phase.

The supervisory control system to modulate the pump movement has been implemented through the NI myRIO module and LabVIEW. MyRIO (My Reconfigurable Input/Output) is a versatile embedded device developed by National Instruments (NI) (Figure 20) that combines a real-time processor and various I/O capabilities into a single compact system. It is designed to provide a platform to develop and prototype a wide range of applications involving data

acquisition, control systems, and signal processing. In terms of I/O capabilities, the myRIO offers a variety of analog and digital input and output channels that can be used to interface with sensors, actuators, and other external devices, enabling users to create systems that interact with the physical world (Figure 21).

Figure 20: data acquisition and control board NI myRIO.

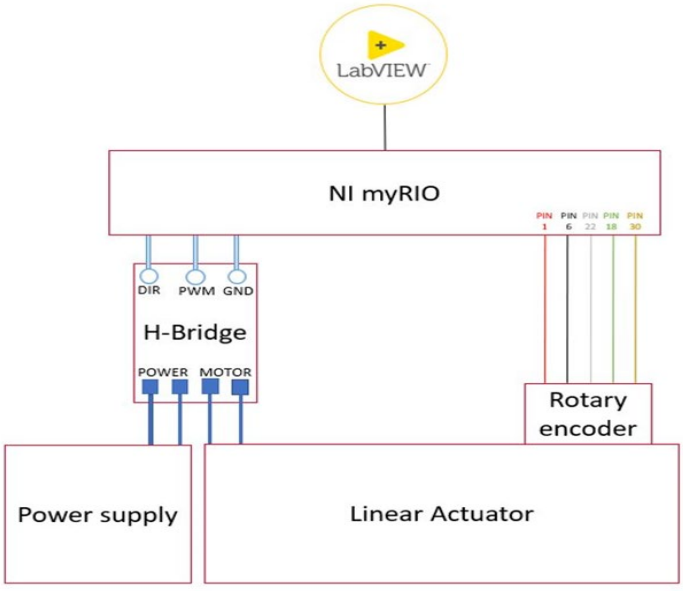

Figure 21: Control system model implemented with NI myRIO.

The supervisory control system has been implemented to induce the linear actuator to reproduce the stroke volume and the heart rate of the human heart and indirectly also end-diastolic volume and end-systolic volume. The myRIO controls the linear actuator movement through an H-bridge circuit (Figure 22). An H-bridge is an electronic circuit configuration commonly used to control the direction and speed of a motor. The myRIO is connected to an MD20A H-bridge with the DIR (myRIO pin 23), PWM (myRIO pin 27), and GRN (myRIO pin 24) H-bridge connectors. In an H-bridge circuit, the GRN (Green or Ground) signal represents the ground or common reference voltage. The DIR (Direction) signal determines the rotational direction of the motor connected to the H-bridge. By controlling the state of the DIR signal, the H-bridge can make the motor rotate in either a clockwise or counter clockwise direction. Finally, the PWM (Pulse Width Modulation) signal is used to control the speed or intensity of a motor or any other device connected to the H-bridge. By adjusting the duty cycle of the PWM signal, the H-bridge can regulate the motor's speed, or the power applied to other devices.

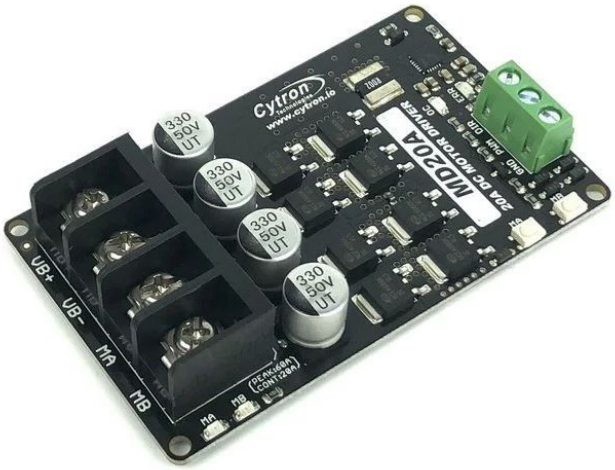

Figure 22:H-bridge.

The H-bridge is powered by a 12V - power supply and converts the digital signal into variable voltage for the motor. The actuator used in this control system is Linak LA12-IC linear actuator (Figure 23). This actuator is suitable for applications requiring short linear movements. The maximum thrust of the device

is 750 N, the maximum speed that can provide is 40 mm/s and the stroke length is 19-130 mm.

The H-bridge is connected to the black and red electrical connections of the linear actuator. The black wire in the Linak LA12-IC actuator is the ground connection. It is connected to the system's ground or reference point, creating a complete circuit for the actuator's electrical operation. The red wire in the Linak LA12-IC actuator represents the positive power supply connection.

Figure 23: Linak LA12-IC actuator.

The linear actuator is embedded with the LPD3806-360BM-G5-24C rotary encoder. The encoder (Figure 24) uses optical sensors to provide signals in the form of discrete pulses which allow linear or rotational movement measurement. By monitoring the pulses generated by the encoder, it is possible to determine the direction of rotation and the number of steps or counts, allowing for relative position measurement.

Figure 24: Rotary Encoder.

This encoder is also connected through the myRIO to the H-bridge displaying the number of rotations calculated. The pulse counter input drives the feedback control system that regulates the movement made by the linear actuator. The encoder is connected to the myRIO through the red (myRIO pin 1), black (myRIO pin 6), green (myRIO pin 18), grey (myRIO pin 30) and white (myRIO pin 22) encoder channels. The Red (Positive or Power) wire represents the positive supply voltage for the encoder. It is connected to the power source, which provides the required voltage level to operate the encoder. The Black (Ground or Common) wire is the ground connection for the encoder. The Green (Channel A) wire is associated with one of the output channels of the encoder. This channel provides the output pulses or signals that are used for position and direction sensing. The Grey wire has been designated as the shielding pin, and its purpose is to provide a path for grounding the shield of the encoder cable. By connecting the shield to ground, it helps minimize the influence of external electromagnetic noise, improving the integrity and accuracy of the encoder signals. Finally, the White (Channel B) is related to the second output channel of the encoder. This channel is also part of the quadrature output and works in conjunction with Channel A. By analyzing the phase relationship between Channel A and Channel B signals, the direction of rotation can be determined. To compute the linear displacement using the LPD3806-360BM-G5-24C rotary encoder, a 0.8 mm lead screw has been connected to the encoder. Then, it has been established the relationship between the rotation of the encoder and the linear movement of the

lead screw. The LPD3806-360BM-G5-24C encoder has a resolution of 360 pulses per revolution, as indicated by the model number. This means that for one full rotation of the encoder shaft, it generates 360 pulses. To determine the linear displacement per pulse, it is necessary to take into account the pitch of the lead screw. The pitch represents the distance the screw moves linearly in one complete revolution. In this case, the lead screw has a pitch of 0.8 mm, meaning it moves 0.8 mm for each complete revolution. Therefore, each pulse generated by the encoder corresponds to a linear displacement of 0.00222 mm (0.8 mm / 360 pulses).

2.1.3 LabVIEW control system

LabVIEW, short for Laboratory Virtual Instrument Engineering Workbench, is a powerful and versatile graphical programming environment developed by National Instruments. LabVIEW allows users to create graphical block diagrams that represent the flow of data and control in their applications. It also provides a wide range of libraries and tools for signal processing, data analysis, and control algorithms.

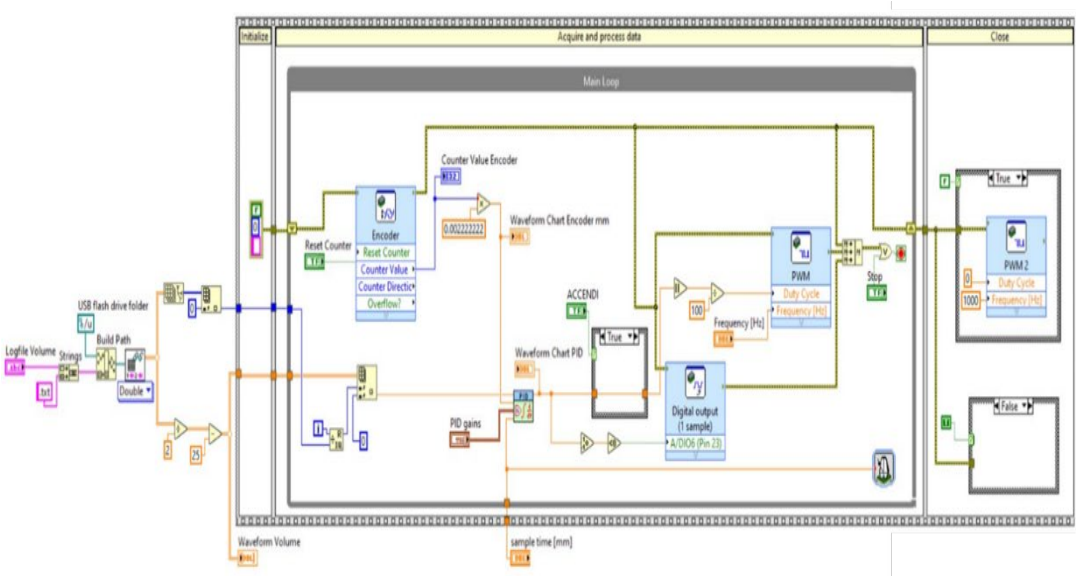

Figure 25: LabVIEW control system.

The control system, depicted in figure 25, has been realized using a feedback logic implemented in LabVIEW through a PID controller. Proportional-Integral-Derivative (PID) controllers[1] 1 are common feedback controllers. In PID control, you specify a process variable and a setpoint. The process variable is the system parameter you want to control and the setpoint is the desired value for that system parameter. A PID controller determines a controller output value and applies the controller output value to the system to drive the process variable toward the setpoint value. The PID controller combines the works by combining the effect of a Proportional (P), Integrative (I), and derivative action. The Proportional (P) action produces an output that is directly proportional to the error between the setpoint and the measured process variable. The larger the error, the larger the corrective action taken. The proportional gain determines the sensitivity of the controller to the error. A higher proportional gain can lead to a faster response but can also result in overshooting the setpoint.

The term sums up past errors and generates an output based on the accumulated error over time. It helps eliminate steady-state errors by gradually reducing the cumulative error. The integral gain determines the rate at which the error is corrected. However, excessive integral gain can introduce instability or cause the system to oscillate. The Derivative action predicts the future behavior of the process variable based on the rate of change of the error. It acts as a damping factor to counteract abrupt changes and minimize overshooting or undershooting the setpoint. The derivative gain affects the response speed and stability of the system. By combining these three terms, the PID controller calculates an output signal that is used to adjust the control variable in order to bring the process variable closer to the setpoint.

[1] The mathematical formulation of a PID control function u(t) is the following:

$$u(t) = K_p e(t) + K_i \int e(t)dt + K_d \frac{de(t)}{dt}$$

where K_p denotes the Proportional gain, K_i denotes the Integrative gain and K_d denotes the Derivative gain. The implementation of this control system requires the tuning of these three constant terms, in order to provide the optimal response.

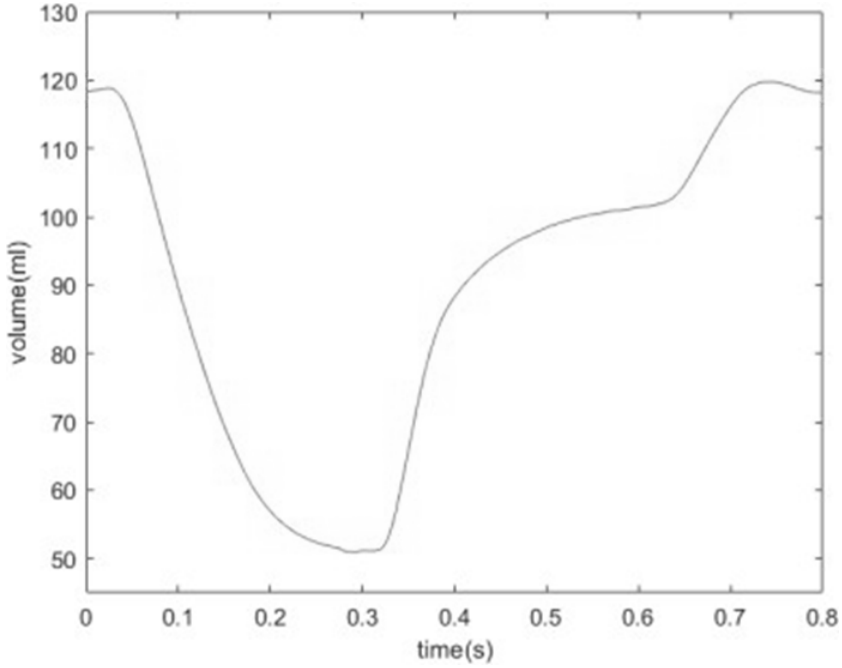

Figure 26: The physiological curve of left ventricular volume in a cardiac cycle [12].

The PID setpoint value, that is the desired value, is a Matlab-generated signal that reflects the instantaneous volume of the left ventricle [12] during an entire cardiac cycle (Figure 26). The purpose of the controller is to move the linear actuator following this waveform. [1] This signal is normalized to improve the performance and stability of the control system. Then it is resized by the Input Array function to send the single sample to the PID. The process variable, which is the parameter that needs to be controlled, derives from the rotary encoder connected to the system.

The encoder data are read by the LabVIEW encoder module and the encoder pulses are converted to linear displacement by multiplying the number of pulses counted by the linear displacement per pulse (0.00222 mm) to obtain the linear displacement. At any given moment, the PID controller will calculate the appropriate control output based on the difference between the process variable and the set point value. The output signal is sent to a LabVIEW case structure that regulates the turning on and off of the actuator. When set the case structure is set to TRUE the motor is activated.

The signal generated by the PID serves to control the Duty Cycle of the waveform that controls the linear actuator. To generate the PWM wave, the PID output signal scale, which ranges from -100 to 100, is changed to the scale 0 to 1. The PWM and DIR signals generated by the controller are the respective outputs of the digital output module function. The PWM signal is delivered from the PWM LabVIEW module (pin 27), while the DIR signal is delivered to the digital output module (pin 23).

These outputs will drive the corresponding control lines of the H-bridge circuit. The entire control system is implemented within a main loop, which continuously reads the encoder data, calculates the error signal, applies PID control, and updates the system. This loop allows for continuous adjustment and control of the system based on the feedback from the encoder. When one of the modules generates a blocking error, the circuit stops passing into the loop close and the engine stops.

2.1.4 Measurement system

Figure 27: myDAQ instrumentation.

To acquire pressure and flow signals the myDAQ instrumentation has been employed. The MyDAQ is a portable data acquisition device developed by National Instruments (Figure 27). It offers analog input and output channels, digital I/O lines, simultaneous sampling, signal conditioning, and software integration. It connects to a computer via USB and is used for acquiring, analyzing, and controlling analog and digital signals in various measurement and control applications.

The measurement system includes the Druck PDCR4011 pressure sensor and the DIGITEN FL-308T electromagnetic flowmeter. The pressure sensor is in left ventricle to acquire the ventricle pressure. This sensor is made up of a membrane integrated with a Wheatstone bridge: the fluid pressure results in a membrane displacement, resulting in a resistance change. The electrical signal resulting from the resistance change is used to quantify the pressure applied to the sensor diaphragm.

The two flow probes enable the flow rate acquisition for the fluid entering the left ventricle and ejected from the ventricle to the aorta. These systems generate a magnetic field and monitor the signal voltage generated by the water as it passes through the tube. According to Faraday's induction law[2], the liquid velocity is derived as a function of the voltage generated by the electrically conductive flow.

The sensors are connected to the analog input channels of MyDAQ, which can accurately measure and sample the electrical signals generated by the sensors. The pressure sensor is alimented with 10 V, while the flow sensors with 5 V (Figure 28).

[2] Faraday's Law.

$$E = k\,B\,D\,V$$

The induced voltage (E) is directly proportional to the velocity (V) of the fluid moving through the magnetic field (B). The transmitter then converts the induced voltage into a quantifiable flow velocity. [9]

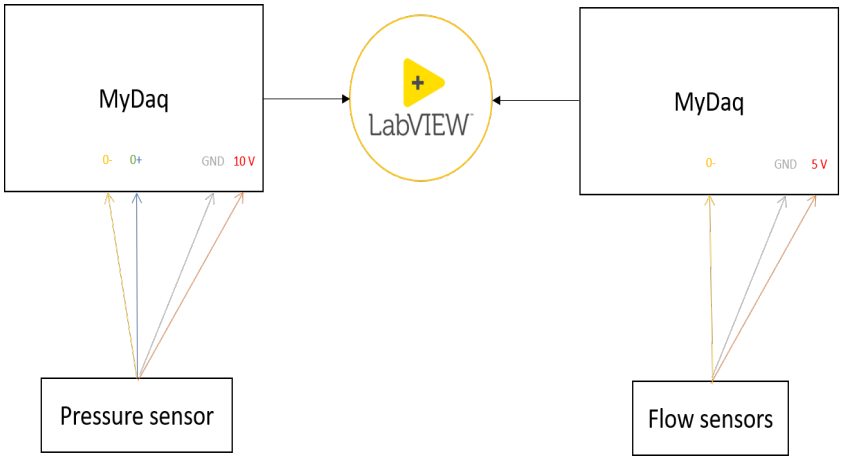

Figure 28: Pressure and flow acquisition implemented with myDAQ.

The pressure and flows signal are calibrated respectively in the following equations (1) and (2):

$$pressure = 11.02 * voltage + 0.791 \quad \text{[mmHg]} \qquad (1)$$

$$flow = 0.094 * frequency + 0.704 \quad \text{[ml/s]} \qquad (2)$$

Then, the signal, derivated and discretized with different samples at different sampling frequencies, is acquired with LabVIEW using myDAQ device (Figure 29). Finally, it is processed using MATLAB.

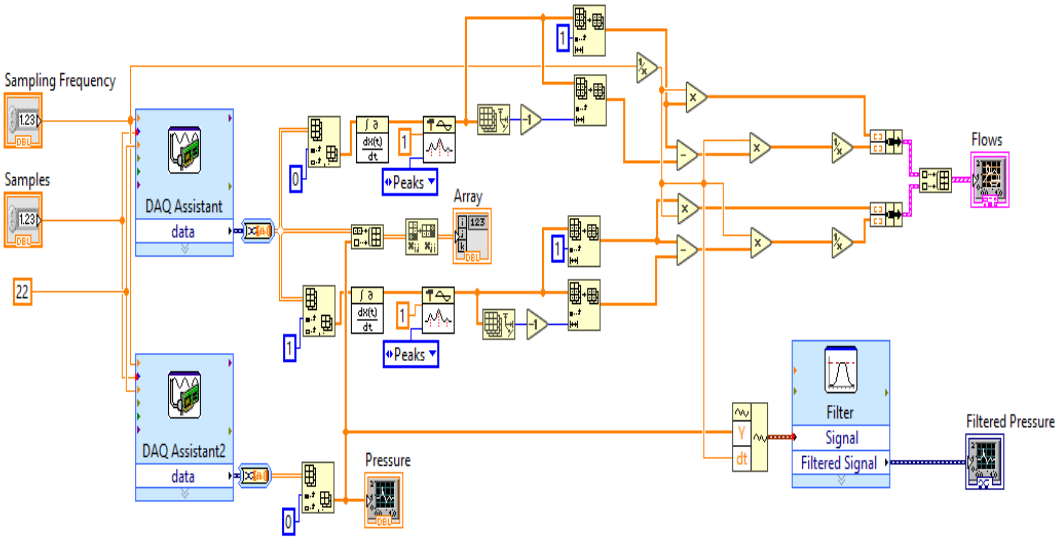

Figure 29: LabVIEW acquisition.

Chapter III

3. Results

Through myRio and LabVIEW, waves waveform volume, waveform chart encoder and waveform chart pid are obtained. Also, the comparison between the waveform volume and the waveform encoder (Figure 30) is computed.

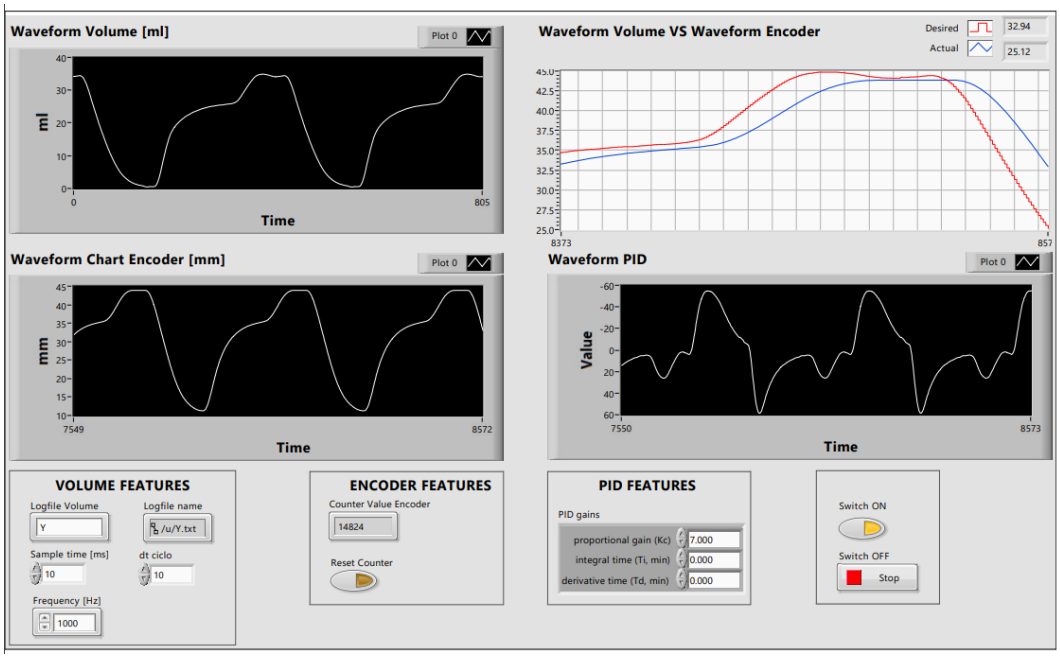

Figure 30: LabVIEW front panel: waveform volume, waveform chart encoder and waveform chart pid. Comparison between the waveform volume and the waveform encoder.

Also, the left ventricle pressure wave is acquired with raw data (Figure 31); then, it is filtered using a Fourier of 2nd order (Figure 32) and lastly the two waves are overlapped (Figure 33).

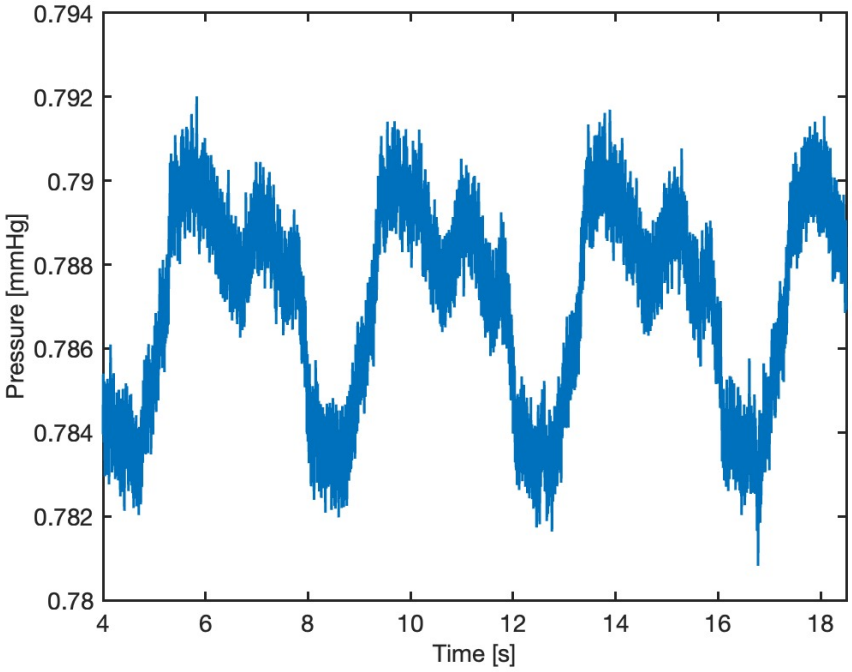

Figure 31: Raw pressure signal

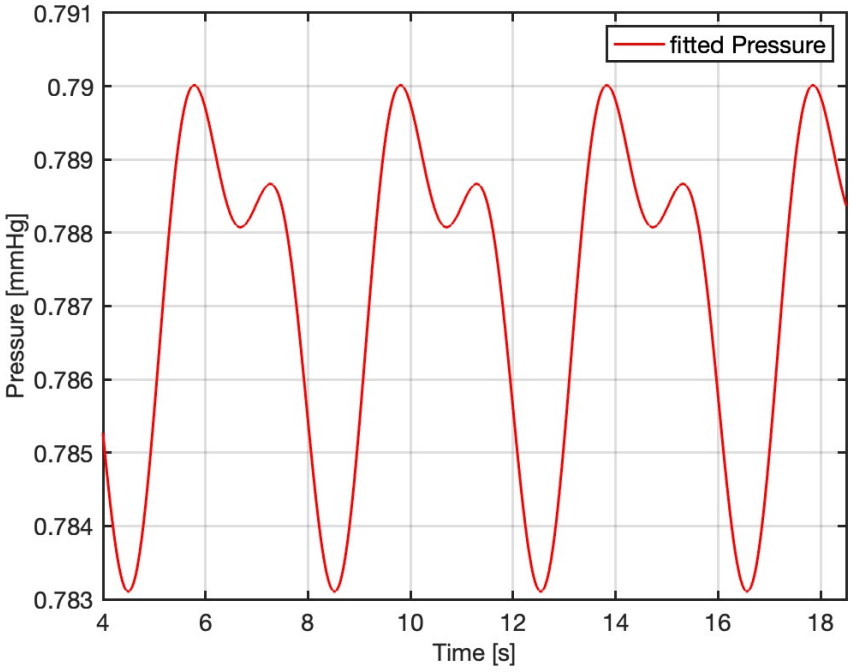

Figure 32: Fitted pressure signal.

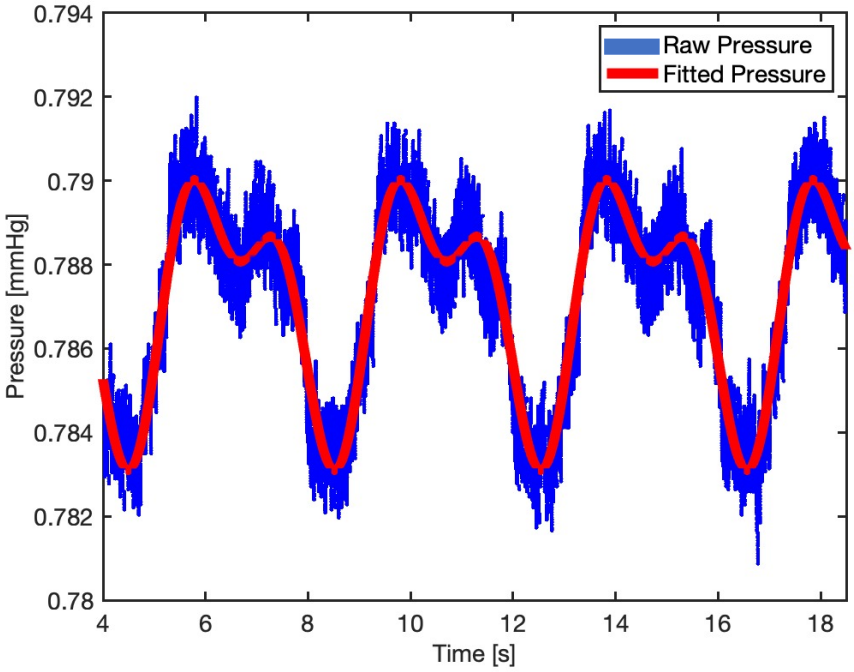

Figure 33: Raw filtered signal in blue and fitted pressure signal in red.

In addition, waves of aortic flow and returned flow were acquired, applying the calibration (Figure 34) and then, also the interpolation (Figure 35).

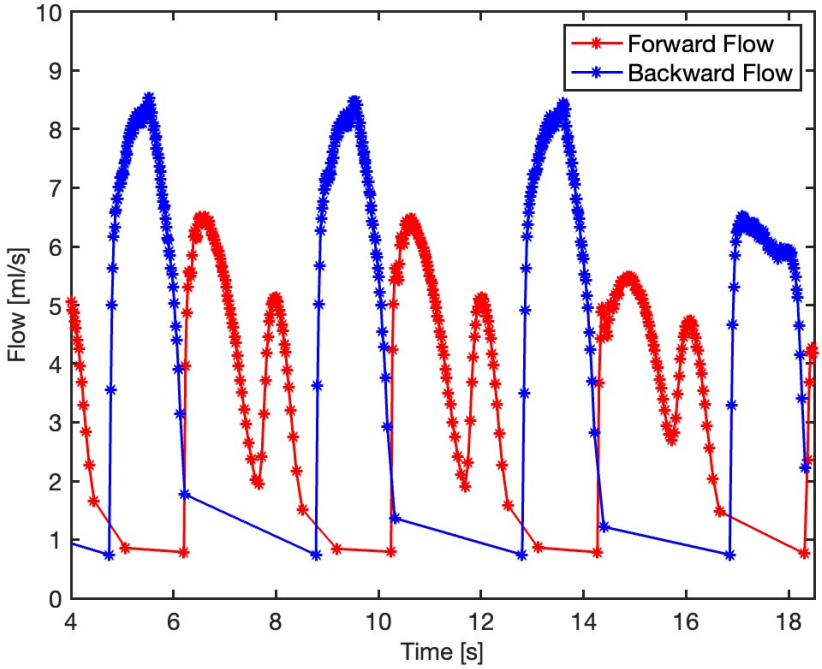

Figure 34: Aortic flow and returned flow acquisition, applying the calibration.

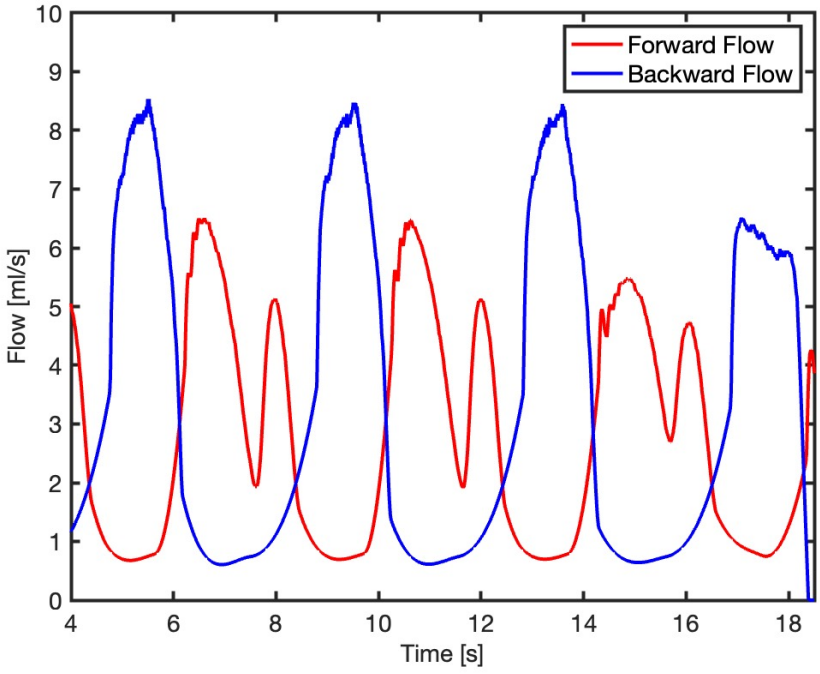

Figure 35: Aortic flow and returned flow acquisition, applying the calibration and interpolation.

Furthermore, waves of aortic flow (Figure 36) and returned flow (Figure 37) were acquired by performing three acquisition tests with the same sampling frequency at 20k Hz.

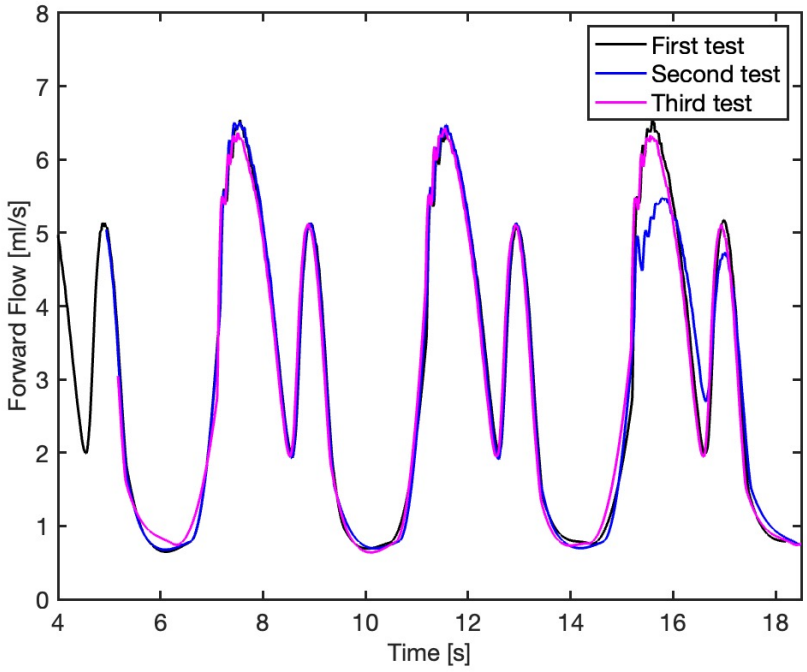

Figure 36: Aortic flow, by performing three acquisition.

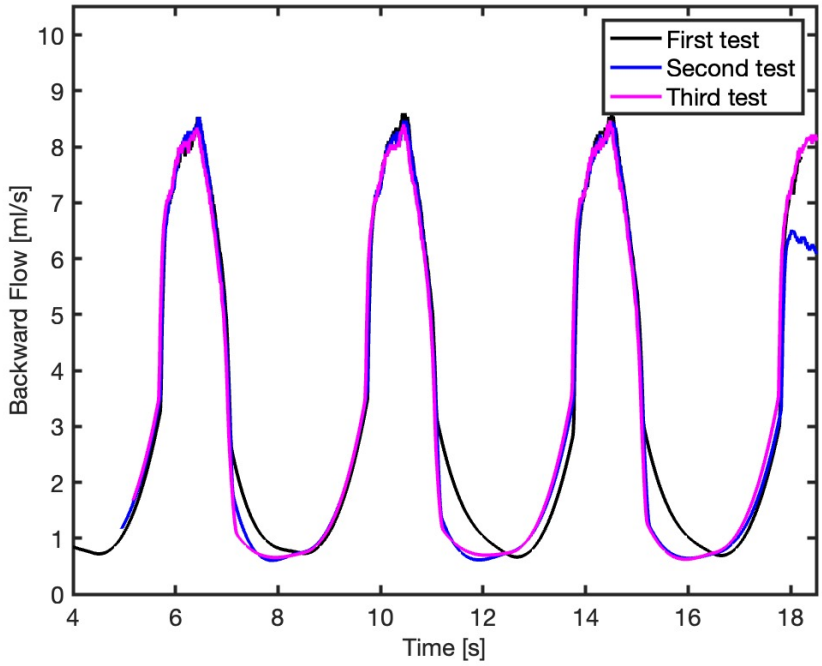

Figure 37: Returned flow, by performing three acquisition.

Then, in order to verify the cardiac simulator ability to replicate ventricular circulation characteristics, the repeatability tests were performed in order to improve the accuracy of the flow rate measurement, using sampling frequency at 5.000 Hz and its zoom of peak (Figure 38-39), at 10.000 Hz and its zoom of peak (Figure 40-41) and then at 15.000 Hz and its zoom of peak (Figure 42-43).

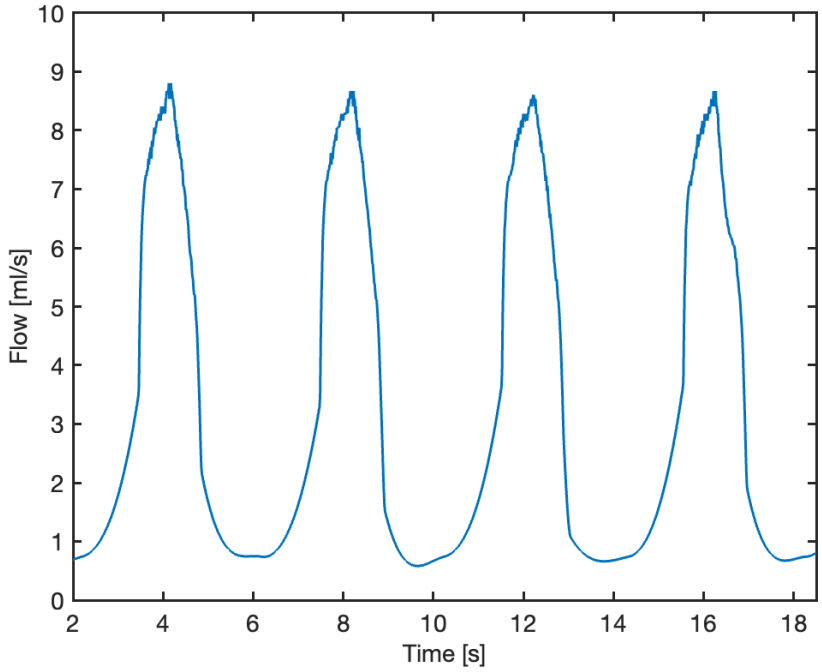

Figure 38: Aortic flow acquisition using sampling frequency of 5.000 Hz.

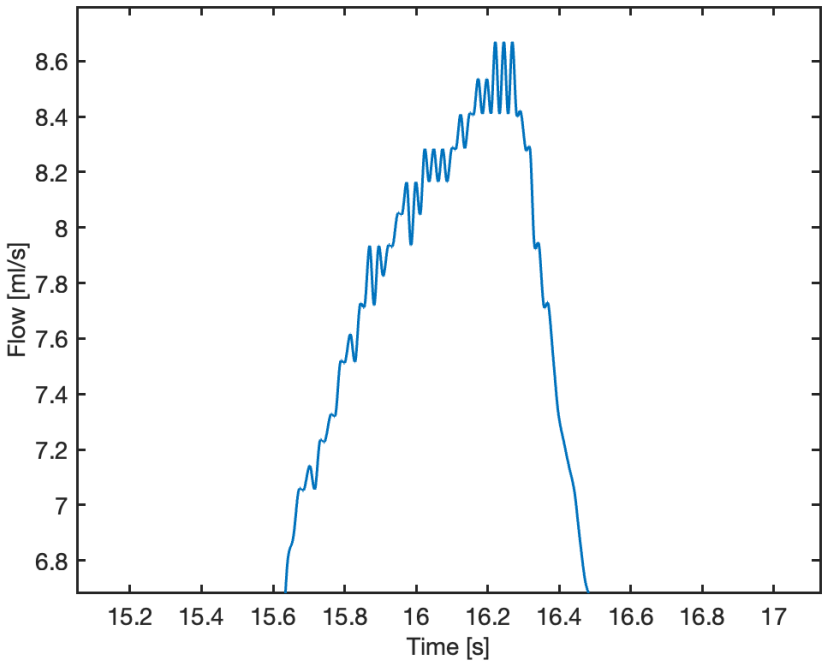

Figure 39: A zoom of the aortic flow acquisition using sampling frequency of 5.000 Hz.

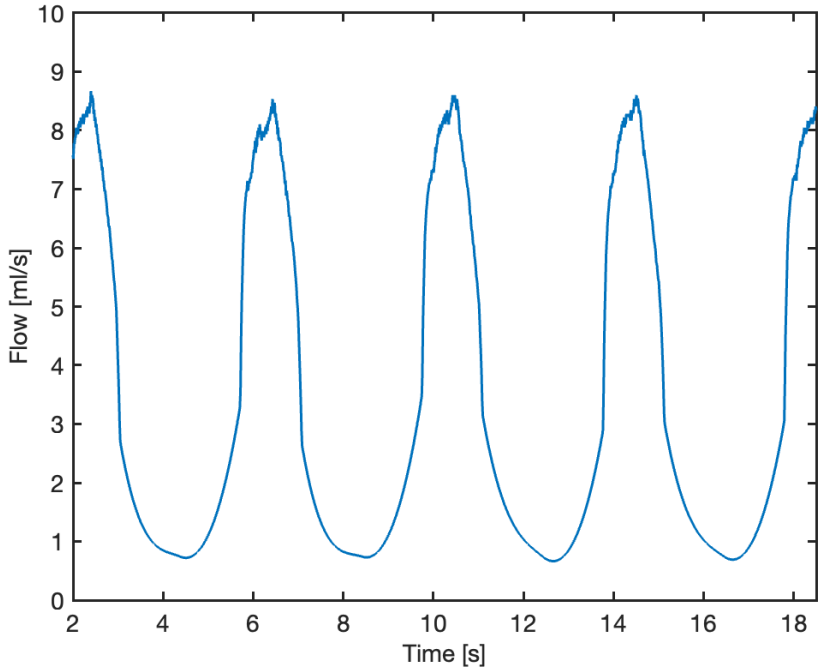

Figure 40: Aortic flow acquisition using sampling frequency of 10.000 Hz.

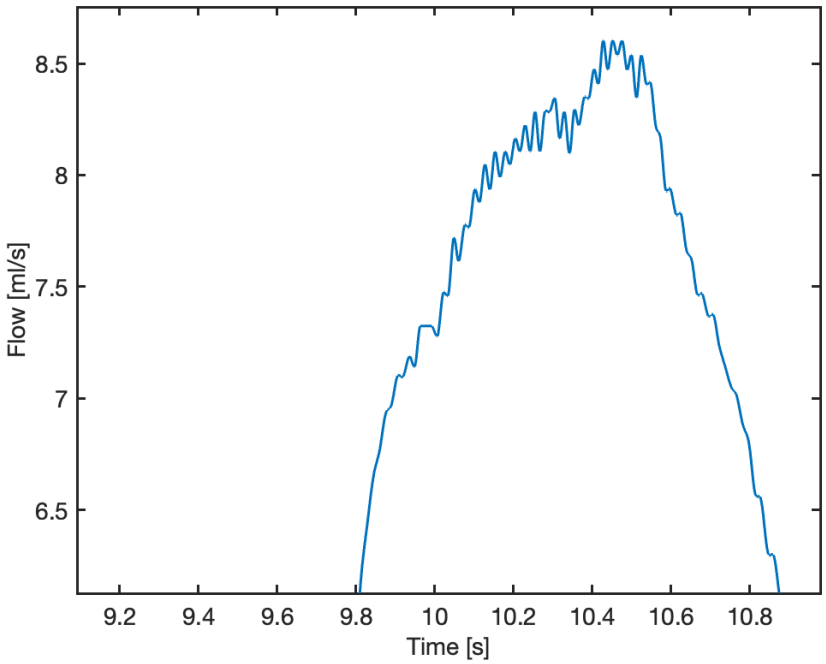

Figure 41: A zoom of the aortic flow acquisition using sampling frequency of 10.000 Hz.

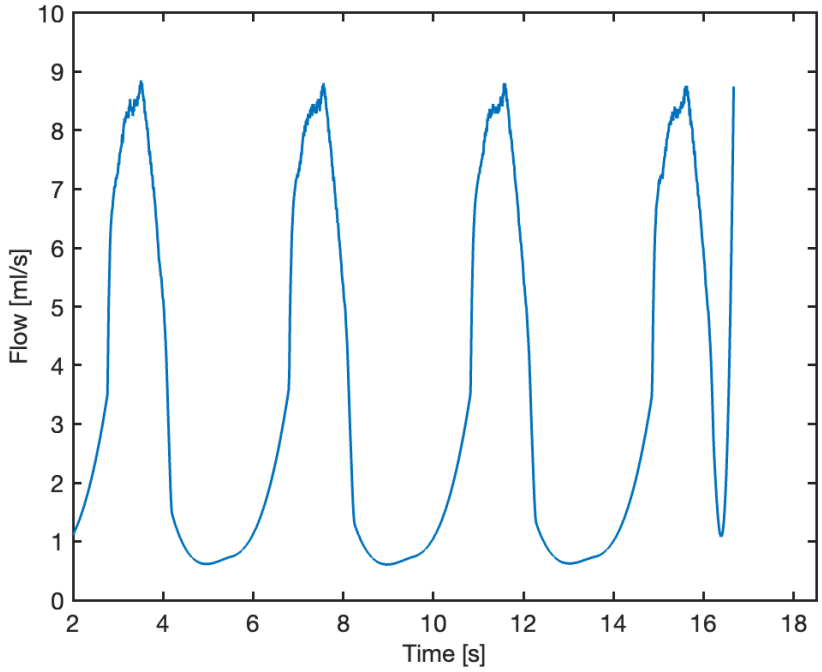

Figure 42: Aortic flow acquisition using sampling frequency of 15.000 Hz.

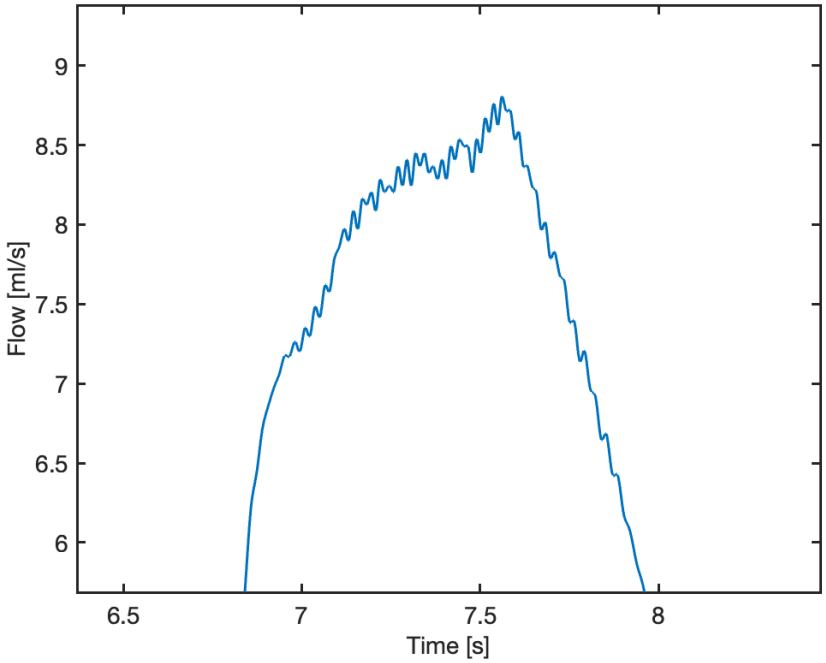

Figure 43: A zoom of the aortic flow acquisition using sampling frequency of 15.000 Hz.

Chapter IV

4. Discussion and conclusions

In recent years, the development of cardiac simulators for prosthetic heart valve testing has become a growing matter of interest in the research field due to several factors. The rising demand for prosthetic heart valves, driven by an aging population and increased prevalence of cardiovascular diseases, necessitates thorough testing to ensure their safety and efficacy. The diverse designs and materials used in manufacturing prosthetic valves require specialized laboratory setups that replicate the complex heart physiological conditions. These simulators enable realistic evaluation of valve function, allowing researchers and manufacturers to facilitate the validation of valve durability and long-term performance, ensuring they can withstand the mechanical stresses of the heart. Under this scenario, the present thesis's purpose was the setup and experimental validation of a cardiac simulator following the same approach that have been carried out in the actual literature. The goal of simulating in vitro the heart pumping activity was the development of a suitable environment for aortic prosthetic heart valve testing. The cardiac simulator consists of a model of the human cardiovascular system whose main elements are a 3D-printed left ventricle membrane and an aortic membrane. To simulate the pulsatile behavior of the heart pumping action the heart model was connected to a linear actuator whose movement has been regulated by a myRio control system. As reported in figure 21, the overall control system is made up of an h-bridge and a rotary encoder, both connected to myRio, that regulate the movement of the linear actuator. In fact, in Figure 30, the comparison between the left ventricle volume wave and the encoder wave shows how the behavior of the two curves are similar, so this result should be important to replicate the physiological movement of the left ventricle.

To evaluate the simulator's performance and validate its accuracy in replicating cardiac parameters, pressure and flowmeters sensors have been employed collected and analyzed using myDaq.

As reported in Figure 33, the acquired raw pressure and the fitted pressure signals follow the trend of left ventricle pressure, considering the diastole and systole of the left ventricle and the subsequent opening and closing of the aortic valve.

As reported in Figure 35, the aortic flow (in red) and the returned flow (in blue) agree with the literature for what concern the behavior of the aortic flow curve in respect to the time.

As reported in Figure 36-37, the aortic and returned flows are acquired by performing three different tests at the same sampling frequency and then, as reported in Figure 38-40-42 the aortic flow is acquired at the different sampling frequencies. The repeatability is done in order to improve the accuracy of the flow rate measurement. In fact, increases the sampling frequency, the accuracy of the wave is higher due to the elevated number of samples, so a better interpolation is computed.

These results suggested that the laboratory test bench that has been realized should be a valid testing system to evaluate the goodness of a prosthetic aortic valve.

Future improvements of this system should be the evaluation of the cardiac simulator response in order to improve adaptation of test bench to physiological functioning of the heart.

In fact, it should be possible vary the aortic valve that has been inserted within the cardiac model; in fact, the chance of evaluating different hemodynamic conditions is of great interest in the field of prosthetic valve replacement.

In addition, alternative solutions could be evaluated in order to improve both the control system and the manufacturing materials chosen for the realization of the considered test bench. A possible solution should be to optimize the control system by better simulating the volume wave and minimizing the errors, playing with PID parameters, time and frequency. So, a complete characterization of the test bench based on a full closed-loop control should be desirable to simulate and vary the heart rate.

Finally, another possible suggestion could be the change the quality of the sensor and/or the position, for example positioning them before and after the aortic valve in order to demonstrate the durability of the valve.

In conclusion, this test bench could be considered as a starting point to provide reliable physiological parameters and curves with the objective to perform several unfailing tests on various types of aortic valves.

Table of figures

References

[1] https://forums.ni.com/t5/labwindows-cvi-user-group/labwindows-cvi-tip-using-the-pid-control-toolkit/ta-p/3531800.

[2] Ovandir Bazan and Jayme Pinto Ortiz. Experimental validation of a cardiac simulator for in vitro evaluation of prosthetic heart valves. Brazilian Journal of Cardiovascular Surgery, 31:151–157, 2016.

[3] Robert M Berne and Matthew N Levy. Principles of physiology. Mosby Incorporated, 2000.

[4] Richard Klabunde. Cardiovascular physiology concepts. Lippincott Williams & Wilkins, 2011.

[5] Patrizio Lancellotti, Philippe Pibarot, John Chambers, Thor Edvard- sen, Victoria Delgado, Raluca Dulgheru, Mauro Pepi, Bernard Cosyns, Mark R Dweck, Madalina Garbi, et al. Recommendations for the imaging assessment of prosthetic heart valves: a report from the european association of cardiovascular imaging endorsed by the chinese society of echocardiography, the inter-american society of echocardiography, and the brazilian department of cardiovascular imaging. European Heart Journal– Cardiovascular Imaging, 17(6):589–590, 2016.

[6] Philip Mathew and Arun Kanmanthareddy. Prosthetic heart valve. 2019.

[7] Matthias C Raschpichler, Felix Woitek, Tarun Chakravarty, Nir Flint, Sung-Han Yoon, Norman Mangner, Chinar G Patel, Chetana Singh, Mohammad Kashif, Philip Kiefer, et al. Valve-in-valve for degenerated transcatheter aortic valve replacement versus valve-in-valve for degenerated surgical aortic bioprostheses: a 3-center comparison of hemodynamic and 1-year outcome. Journal of the American Heart Association, 9(14): e013973, 2020.

[8] Marco Russo, Maurizio Taramasso, Andrea Guidotti, Alberto Pozzoli, Fabian Nietilspach, Ludwig Von Segesser, and Francesco Maisano. The evolution of surgical valves. Cardiovascular Medicine, 20(12):285–292, 2017.

[9] John G Webster. Medical instrumentation: application and design. John Wiley & Sons, 2009.

[10] Ke-Wei Xu, Qi Gao, Min Wan, and Ke Zhang. Mock circulatory loop applications for testing cardiovascular assist devices and in vitro studies. Frontiers in Physiology, 14:621, 2023.

[11] Querzoli, G., Fortini, S., Espa, S., & Melchionna, S. (2016). Un modello di laboratorio del flusso della radice aortica comprese le arterie coronarie. Esperimenti sui fluidi, 57, 1-9.

[12] Guyton AC, Hall JE. Textbook of medical physiology. 11th Ed. Philadelphia: Elsevier Inc.; 2006. Heart muscle; the heart as a pump and function of the heart valves; pp. 103–115.